# Subduction or sagduction? Ambiguity in constraining the origin of ultramafic–mafic bodies in the Archean crust of NW Scotland

Tim E. Johnson[a*], Michael Brown[b], Kathryn M. Goodenough[c], Chris Clark[a], Peter D. Kinny[a] & Richard W. White[d]

[a] *Department of Applied Geology, The Institute for Geoscience Research (TIGeR), Curtin University, GPO Box U1987, Perth WA 6845, Australia*

[b] *Laboratory for Crustal Petrology, Department of Geology, University of Maryland, College Park, MD 20742-4211, USA*

[c] *British Geological Survey, West Mains Road, Edinburgh EH9 3LA, UK*

[d] *Earth System Science Research Centre, Institute for Geosciences, University of Mainz, Becherweg 21, D–55099, Mainz, Germany*

Corresponding author at: Department of Applied Geology, Curtin University, GPO Box U1987, Perth WA 6845, Australia.

Tel.: +61 8 92667332; fax: +61 8 92663153

*E-mail address:* tjohnson@uni-mainz.de (Tim Johnson)

Running title: LEWISIAN ULTRAMAFIC–MAFIC BODIES

**ABSTRACT**

The Lewisian Complex of NW Scotland is a fragment of the North Atlantic Craton. It comprises mostly Archean tonalite–trondhjemite–granodiorite (TTG) orthogneisses that were variably metamorphosed and reworked in the late Neoarchean to Palaeoproterozoic. Within the granulite facies central region of the mainland Lewisian Complex, discontinuous belts composed of ultramafic–mafic rocks and structurally overlying garnet–biotite gneiss (brown gneiss) are spatially associated with steeply-inclined amphibolite facies shear zones that have been interpreted as terrane boundaries. Interpretation of the primary chemical composition of these rocks is complicated by partial melting and melt loss during granulite facies metamorphism, and contamination with melts derived from the adjacent migmatitic TTG host rocks. Notwithstanding, the composition of the layered ultramafic–mafic rocks is suggestive of a protolith formed by differentiation of tholeiitic magma, where the ultramafic portions of these bodies represent the metamorphosed cumulates and the mafic portions the metamorphosed fractionated liquids. Although the composition of the brown gneiss does not clearly discriminate the protolith, it most likely represents a metamorphosed sedimentary or volcano-sedimentary sequence. For Archean rocks, particularly those metamorphosed to granulite facies, the geochemical characteristics typically used for discrimination of paleotectonic environments are neither strictly appropriate nor clearly diagnostic. Many of the rocks in the Lewisian Complex have ‘arc-like’ trace element signatures. These signatures are interpreted to reflect derivation from hydrated enriched mantle and, in the case of the TTG gneisses, partial melting of amphibolite source rocks containing garnet and a Ti-rich phase, probably rutile. However, it is becoming increasingly recognized that in Archean rocks such signatures may not be unique to a subduction environment but may relate to processes such as delamination and dripping. Consequently, it is unclear whether the Lewisian ultramafic–mafic rocks and brown gneisses represent products of plate margin or

intraplate magmatism. Although a subduction-related origin is possible, we propose that an intraplate origin is equally plausible. If the second alternative is correct, the ultramafic–mafic rocks and brown gneisses may represent the remnants of intracratonic greenstone belts that sank into the deep crust due to their density contrast with the underlying partially molten low viscosity TTG orthogneisses.

## 1. Introduction

Archean cratons are predominantly composed of lower-grade granite–greenstone belts and higher-grade grey gneiss terrains that may represent the upper and lower levels of ancient continental crust (Windley and Bridgewater, 1971). In an alternative view, the high-grade gneiss complexes and granite–greenstone belts have been interpreted as the ancient analogues of modern active continental margins and back-arcs, respectively (Windley and Smith, 1976). These different interpretations persist to the present day and are reflected in the 'subduction versus sagduction' controversy for the formation of particular fragments of Archean crust, such as the Barberton granite–greenstone belt (e.g., Kisters et al., 2003, 2010; Van Kranendonk et al., 2014; Brown, 2015; Cutts et al., 2015).

Greenstone belts are linear to irregular in shape and generally synformal in structure, comprising volcano-sedimentary successions (De Wit and Ashwal, 1997) that are surrounded by dome-like composite batholiths of gneiss and granite (McGregor, 1951; Anhaeusser, 1975, 2014). Although lithologically complex and diverse in detail, greenstone belts are dominated by (metamorphosed) basalt with other volcanic rocks ranging in composition from ultramafic (komatiite) to felsic (dacite–rhyolite) and various sedimentary rocks that generally become more abundant at shallower levels (Condie, 1994; De Wit and Ashwal, 1997;

Eriksson et al., 1997; Sylvester et al., 1997; Anhaeusser, 2014). Layered ultramafic–mafic bodies may occur near the base of greenstone belts (Anhaeusser, 1975, 2001, 2014), which has led some to interpret greenstone belts as dismembered fragments of obducted Archean oceanic crust (ophiolites) and hence as evidence of subduction (De Wit et al., 1987; Kusky, 1990; Furnes et al., 2009; Hickman, 2012).

Grey gneiss terrains are dominated by felsic orthogneisses metamorphosed at amphibolite to granulite facies, of which most (~70–75 vol.%) are tonalitic, trondhjemitic or granodioritic (TTG) in composition (Moyen, 2011; Moyen and Martin, 2012). Commonly, grey gneiss terrains include highly deformed layered ultramafic–mafic bodies and supracrustal belts dominated by metavolcanic rocks. This association of rock types has been interpreted by some to result from the dismemberment of oceanic island arcs formed at convergent plate margins (e.g. Polat et al., 2015).

Although the archetypical dome-and-basin structure of Archean upper crust has been regarded to be the result of polyphase folding during subhorizontal shortening (i.e. accretion; e.g. Myers & Watkins, 1985; Blewett et al., 2002), this structure is more commonly interpreted to reflect sinking, or 'sagduction' (Goodwin and Smith, 1980), of the overlying greenstones and diapiric rise of gneisses and granitic plutons (Anhaeusser, 1975, 2014; Brun, 1980; Brun et al., 1981; Ramsay, 1989; Bouhallier et al., 1995; Kisters & Anhaeusser, 1995; Chardon et al., 1996, 1998; Collins et al., 1998; Bremond d'Ars et al., 1999; Marshak, 1999; Wellman, 2000; Sandiford et al., 2004; Van Kranendonk et al., 2004, 2014; Parmenter et al., 2006; Robin and Bailey 2009; Thebaud and Rey 2013; François et al., 2014; Gapais et al., 2014; Brown, 2015; Sizova et al., 2015). In many cases, rocks within grey gneiss terrains have undergone polyphase deformation coeval with high-grade metamorphism at suprasolidus conditions (Horie et al., 2011; Johnson et al., 2012, 2013). As a result, establishing the relationship between the different lithological components, the origin of their protoliths and the tectonic style poses challenges. However, if the dome-and-basin structure of low-grade (greenschist to amphibolite facies) granite–greenstone terrains does reflect diapirism and sagduction, then the disrupted remnants of the sinking greenstone belts might be expected to occur in high-grade (amphibolite to granulite facies) gneiss terrains that represent deeper levels in the Archean crust.

The evidence for subduction in the early Earth is based to a large degree on the ‘arc-like’ geochemical signature preserved by many Archean volcanic rocks. Such signatures indicate the rocks were derived from fluid-fluxed melting of mantle enriched in large-ion lithophile elements (LILE) but depleted in high field-strength elements (HFSE), which is commonly interpreted to record dehydration and/or partial melting of the downgoing slab and concomitant enrichment of the overlying mantle wedge during subduction (e.g. Tatsumi, 2005; Jenner et al., 2009). However, it is becoming increasingly recognised that ‘arc-like’ signatures may be generated in other geodynamic scenarios (Pearce, 2008; van Hunen and Moyen, 2012) in which hydrated and enriched supracrustal material (e.g. sediment) is transferred to the upper mantle. Recent geodynamic models for the early Earth, when the mantle was much hotter, suggest that such non-uniformitarian scenarios are plausible alternatives to subduction (Johnson et al., 2014; Sizova et al., 2015).

We use field observations combined with bulk-rock major oxide and trace element compositional data to examine the origin of ultramafic–mafic–supracrustal bodies from the Lewisian Complex of NW Scotland. An origin by subduction–accretion (‘horizontal tectonics’) or by partial convective overturn (‘vertical tectonics’) is permissible within the limitations of the data and the context of our current understanding of Archean crustal dynamics. In these circumstances, resolution of the origin of the rocks comprising Archean high-grade gneiss terrains may only be possible using geodynamic modelling informed by the available geological data.

## 2. Geological setting

The Lewisian Complex of NW Scotland is a classic Precambrian high-grade grey gneiss terrain. The rocks are mostly orthogneisses with Mesoarchean to Neoarchean protolith ages that record a protracted history of magmatism, deformation and metamorphism spanning more than a billion years (Kinny et al., 2005; Wheeler et al., 2010; Goodenough et al., 2013; Crowley et al., 2015; Macdonald et al., 2015; Mason et al., 2015). The complex is dominated by TTG gneisses within which occur abundant bodies of metamorphosed ultramafic–mafic rocks and, locally, mica- and garnet-rich gneisses (Peach et al., 1907). The ultramafic–mafic bodies range in shape and size from layered units several hundred metres across and several kilometres in length to smaller metre-scale sheets and pods a few centimetres in diameter (e.g. Bowes et al., 1964; Davies 1974; Sills et al., 1982; Rollinson & Fowler, 1987; Johnson et al., 2012).

On the mainland, the Lewisian Complex comprises a granulite facies central region bounded by regions to the north and south that record mainly amphibolite facies conditions (Peach et al., 1907; Sutton and Watson, 1951; Fig. 1). Traditionally, the central region has been interpreted to represent the deeper levels of a once-contiguous crustal block (e.g. Sheraton et al., 1973; Park and Tarney, 1987). However, more recently, based on geochronological studies, it has been proposed that the Lewisian Complex represents several discrete crustal blocks (terranes) bounded by major shear zones, although the number of terranes, the position of the terrane boundaries and the timing of their assembly is debated (Kinny and Friend, 1997; Park et al., 2001; Kinny et al., 2005; Park, 2005; Goodenough et al., 2010, 2013). To avoid any genetic connotations, we hereafter refer to the different mainland ‘terranes’, as documented in Kinny et al. (2005), as ‘blocks’, following the usage of Crowley et al. (2015).

In this section we review information pertaining to rocks in the central region (comprising the Gruinard block in the south and the Assynt block in the north; Love et al., 2004; Fig. 1) and describe the relationship between the northern part of the central region (Assynt block) and the northern region (Rhiconich block; Kinny et al., 2005) across the Laxford Shear Zone (Goodenough et al., 2010, 2013), where abundant large ultramafic–mafic bodies and associated supracrustal rocks have been mapped in detail (BGS map sheets NC14 and NC24; Davies, 1976; see Fig. 2). Temporal constraints are summarised in Fig. 3. These provides a foundation for the following two sections in which we provide details of the field relations and chemical compositions of the ultramafic–mafic bodies and supracrustal rocks occurring within the central region.

### *2.1. Central region—protoliths and granulite facies (Badcallian) metamorphism*

Away from shear zones, central region TTG gneisses are characterised by a shallow- to moderate-dipping gneissosity and recumbent tight-to-isoclinal folds (Wheeler et al., 2010). The TTG gneisses preserve anhydrous (two pyroxene) mineral assemblages related to the granulite facies metamorphic event (Badcallian; Park, 1970), which are variably overprinted by amphibolite facies assemblages in which clinopyroxene and orthopyroxene are replaced by hornblende and biotite, respectively.

Metabasic rocks preserve a variety of granulite facies mineral assemblages, with many containing, in addition to pyroxenes and plagioclase, brown (Ti-rich) hornblende and/or abundant garnet as part of the peak metamorphic mineral assemblage. Ultramafic rocks are characterised by peak assemblages containing olivine, orthopyroxene, clinopyroxene, brown hornblende and spinel, whose relative proportions vary (Johnson and White, 2011). The mineral assemblages in this range of rock types are consistent with peak metamorphic conditions of $P$ = 0.8–1.2 GPa at $T$ of >900 °C (Barnicoat, 1983; Cartwright and Barnicoat, 1987; Sills and Rollinson, 1987; Johnson and White, 2011; Zirkler et al., 2012; Johnson et al., 2013). Plagioclase, orthopyroxene and magnetite coronae replacing garnet in metabasic rocks are interpreted to record limited near-isothermal retrograde decompression to 0.7–0.9 GPa (Johnson & White, 2011). The absence of garnet in metamorphosed ultramafic rocks, and the lack of evidence for its presence during prograde metamorphism, suggests the rocks did not reach pressures higher than those recorded at the metamorphic peak. Combined, these data are consistent with $P$–$T$ paths that are tight clockwise loops in which peak $T$ coincided with peak $P$ (Johnson and White, 2011, fig. 5b).

With the exception of ultramafic and rare calc-silicate rocks, granulite facies metamorphism resulted in extensive partial melting and loss of melt (Johnson et al., 2012, 2013). Central region TTG gneisses show a distinctive depletion of large ion lithophile and other mobile elements relative to rocks from the northern and southern regions (e.g. Sheraton et al., 1973; Johnson et al., 2013, fig. 2). This depletion was related to the high-grade metamorphism (Moorbath et al., 1969), with removal of mobile elements via the loss of partial melt (O'Hara and Yarwood, 1978; Pride and Muecke, 1980, 1982; Cohen et al., 1991; Johnson et al., 2012, 2013), although some of the differences reflect heterogeneities in the original source composition (Rollinson and Tarney, 2005; Rollinson, 2012; Hughes et al., 2014).

Around Scourie, Badcall and Kylestrome (Assynt block; Fig. 1), based on SHRIMP U–Pb dating of zircon, the TTG gneisses have protolith (crystallisation) ages as old as *c.* 3.03–2.96 Ga (Friend and Kinny, 1995; Kinny and Friend, 1997), consistent with Sm–Nd systematics (Hamilton et al., 1979). However, based on SIMS, SHRIMP and TIMS U–Pb dating on zircon, younger protolith ages of *c.* 2.86-2.85 Ga have been suggested for some gneisses within the Assynt block (Whitehouse and Kemp, 2010; Goodenough et al., 2013; Crowley et al., 2015; Figs 2,3), which are similar to ages of *c.* 2.86–2.79 Ga inferred for gneisses further south within the Gruinard block (Whitehouse et al., 1997; Corfu et al., 1998; Love et al., 2004; Fig. 1).

The peak of Badcallian metamorphism in the Assynt block is inferred by some to have occurred at *c.* 2.8–2.7 Ga (Fig. 3), based on TIMS U–Pb data from zircon (Corfu et al., 1994) and *in situ* SIMS Pb–Pb data from a monazite inclusion in garnet (Zhu et al., 1997). Others place the peak of high-grade metamorphism in the Assynt block at *c.* 2.49–2.48 Ga, based on SHRIMP U–Pb data from zircon in the area north of Lochinver (Friend and Kinny, 1995; Kinny and Friend, 1997; Figs 1, 3). Corfu (2007) interprets these two groups of ages as recording separate metamorphic events, which he correlated with the Badcallian and Inverian (see below), respectively. Notwithstanding these interpretations, several studies have indicated that samples of TTG gneiss from the Assynt block show a smear of zircon ages along concordia between *c.* 3.0 and 2.5 Ga, in which individual metamorphic events are difficult to identify (e.g. Whitehouse and Kemp, 2010), possibly reflecting variable Pb loss from zircon during deformation and/or protracted cooling (e.g. Ashwal et al., 1999; MacDonald et al., 2013). In a recent study using a technique involving partial dissolution of thermally annealed morphologically complex zircon grains analysed by ID–TIMS, Crowley et al. (2015) provide evidence in support of two high-grade metamorphic events in the Assynt block, at *c.* 2.7 Ga and *c.* 2.5 Ga.

The peak of granulite facies metamorphism in the strongly retrogressed gneisses further south in the central region, within the Gruinard block, is considered to have occurred at c. 2.73 Ga (TIMS and SHRIMP U-Pb on zircon; Corfu et al., 1998; Love et al., 2004), with no evidence for any later (c. 2.5 Ga) high-grade event. This led Corfu et al. (1998) to argue that the Assynt and Gruinard blocks expose different levels of a once-contiguous crustal fragment, and Love et al. (2004) to suggest that the Assynt and Gruinard blocks represent discrete terranes.

*2.2. Post-Badcallian evolution and the relationship between the central and northern regions*

At the northern margin of the central region is the Laxford Shear Zone (LSZ), a several kilometre wide WNW-trending, steeply south-dipping ductile shear zone involving complex polyphase deformation and metamorphism that has been proposed to be an early Proterozoic terrane boundary (Kinny and Friend, 1997; Friend and Kinny, 2001; Kinny et al., 2005; Goodenough et al., 2010, 2013; Fig. 2). Within the LSZ and throughout the central region, reworking of the granulite-facies gneisses is related to two separate post-Badcallian tectonometamorphic events (Goodenough et al., 2010; Wheeler et al., 2010).

A series of steep NW–SE- to WNW–ESE-trending shear zones (Evans and Lambert, 1974; Coward and Park, 1987; Wheeler, 2007) is inferred to have developed during the Inverian event (Evans 1965). Inverian metamorphism was associated with pervasive retrogression of granulite facies assemblages, but only limited partial melting and magmatism. These Inverian shear zones contain kinematic indicators consistent with dominant bulk horizontal shortening (thrusting) with a small dextral component (Beach et al., 1974; Coward and Park, 1987) that could explain juxtaposition of the central region granulites over the lower-grade rocks of the northern region (Coward 1984, 1990; Wheeler et al., 2010) and, furthermore, could have provided a potential source of the fluid required for retrogression (Beach, 1980). *P*–*T* estimates for the Inverian event are 500–625 °C and 0.50–0.65 GPa (Sills, 1983; Cartwright et al., 1985; Sills and Rollinson, 1987; Zirkler et al., 2012).

Pegmatites in the Lochinver and Scourie areas have been dated at *c*. 2.48 Ga (TIMS U–Pb on zircon, Corfu et al., 1994; *in situ* SIMS Pb–Pb on monazite, Zhu et al., 1997). Goodenough et al. (2013) report LA–ICPMS U–Pb ages from zircons within a folded and foliated microgranite from Tarbet of 2.48 Ga and 1.76 Ga, which they interpret to date metamorphism correlated with the Inverian and Laxfordian events (see below), respectively (Fig. 3).

Inverian deformation and metamorphism was followed by emplacement of a suite of mafic and ultramafic dykes (the Scourie Dykes; Peach et al., 1907; Sutton and Watson, 1951). Most of the dykes were intruded in the interval 2.42–2.37 Ga (U–Pb baddeleyite and zircon ages, Davies and Heaman, 2014; Fig. 3) and are inferred to have been derived largely from partial melting of metasomatically-enriched sub-continental mantle lithosphere (Hughes et al., 2014). Hughes and co-workers suggest this enrichment may be related to subduction during the late Archean.

Post-Scourie Dyke reworking associated with amphibolite facies metamorphism is related to the late Paleoproterozoic Laxfordian event (Sutton and Watson, 1951; Goodenough et al., 2010). In the central region, north of Scourie (Assynt block), retrogressed granulites are cut by discrete metre-scale E–W-trending shear zones that deform and offset the Scourie Dykes (Beach et al., 1974; Coward, 1990). These shear zones increase in abundance and swing into a NW–SE orientation approaching the LSZ. Coward (1990) interpreted the large-scale structures to indicate early Laxfordian dextral thrusting, although this deformation may have been Inverian in age (Goodenough et al., 2010). Later sinistral extension (Beach et al., 1974) was interpreted by Coward (1990) as due to Laxfordian reactivation of earlier structures. Fluid ingress along amphibolite facies Laxfordian shear zones led to the generation and intrusion of voluminous granite as dykes, and metasomatic alteration of both Scourie Dykes and the TTG gneisses (Beach and Fyfe, 1972; Beach, 1973, 1976, 1980).

Zircons from a pre- to syn-Laxfordian granite from Ben Stack yielded an LA–ICP–MS U–Pb age of 1.88 ± 0.2 Ga whereas those from an undeformed (post-Laxfordian) granitic pegmatite from Badnabay gave an ID–TIMS U–Pb age of 1.77 ± 0.001 Ga (Goodenough et al., 2013). A SHRIMP U–Pb zircon age of 1.854 ± 0.13 Ga was obtained from a composite granite–pegmatite sheet just to the north of the LSZ (Friend and Kinny, 2001).

### *2.3. Layered ultramafic–mafic bodies and metasedimentary rocks*

Layered ultramafic–mafic bodies, some several hundred metres in thickness, are widely distributed across the central region, together constituting perhaps 5–10% of the total outcrop (e.g. Peach et al., 1907; O'Hara 1961; Bowes et al., 1964; Davies, 1974; Sills et al., 1982; Burton et al., 2000; Johnson et al., 2012; Fig. 2). Although generally sheet-like, the larger layered bodies define open to isoclinal, upright to near-recumbent synforms (Davies, 1974; Cartwright et al., 1985), the cores of which are locally occupied by quartzo-feldspathic garnet–biotite gneiss (hereafter brown gneiss; Sutton and Watson, 1951). In the literature these brown gneisses have been interpreted as sedimentary in origin (e.g. Beach, 1974; Cartwright et al., 1985; Cartwright and Barnicoat, 1987), but they could be volcanogenic (discussed below); in either case, the spatial relationship suggests that the synforms are synclines (Davies, 1974).

At their margins most of the ultramafic–mafic bodies are steeply inclined and appear to be concordant with an intense steeply dipping fabric in the surrounding TTG gneisses that is most intense at the contact with these bodies. These steeply dipping gneisses are retrogressed to amphibolite facies, meaning that the marginal shear zones are Inverian (or Laxfordian or a combination of both events) by definition (Evans, 1965), although the time at which this steep fabric originally formed is uncertain.

The most extensive outcrops of layered ultramafic–mafic rocks and brown gneisses occur in the north of the central region, towards the southern margin of the LSZ, where these lithologies define a tightly folded belt up to a kilometre or more in width and extending for more than 12 km along strike (Davies, 1974; Goodenough et al., 2010; Fig. 2). In addition, layered ultramafic–mafic bodies crop out throughout the central region, particularly good examples occurring on the flanks of Ben Strome (north-east of Kylesku) and close to the villages of Scourie, Drumbeg and Achiltibuie (e.g. O'Hara, 1961; Bowes et al., 1964; Sills et al., 1982; Johnson et al., 2012; Figs 1 and 2). Furthermore, smaller ultramafic and mafic bodies are ubiquitous within the central region granulites, occurring as disrupted sheets and pods several metres across down to centimetre-size remnants. The large ultramafic–mafic bodies have major oxide, trace element and isotopic compositions suggesting they were derived from MgO-rich (15–20 wt %) tholeiitic melts (Sills et al., 1982; Burton et al., 2000).

Mafic and ultramafic rocks have Sm–Nd whole rock ages of *c.* 3.0–2.7 Ga (e.g. Whitehouse, 1989; Cohen et al., 1991; Whitehouse et al., 1996; Fig. 3); an age of 2.707 ± 0.052 Ga is interpreted as the time of igneous differentiation of the ultramafic–mafic bodies (Cohen et al., 1991). Ultramafic–mafic rocks yield a Re–Os age of 2.686 ± 0.15 Ga (MSWD = 1.43 and initial $^{187}Os/^{188}Os$=0.10940 ± 0.00076; Burton et al., 2000), interpreted by these authors as the time of emplacement of the ultramafic–mafic bodies. However, there is evidence for post-emplacement perturbation of both Sm–Nd and Re–Os isotopic systems (Whitehouse et al., 1997; Burton et al., 2000). Zircon in a hornblendite from the Gruinard block with a SIUMS U–Pb age of *c.* 2.8 Ga is interpreted to date metamorphism (Whitehouse et al., 1997).

U–Pb zircon ages from samples of brown gneiss (LA-MC-ICP-MS and ID-TIMS, Goodenough et al., 2013) and a rare white-mica gneiss (LA-MC-ICP-MS, Zirkler et al., 2012) give a spread of ages along concordia from *c.* 2.8 to *c.* 2.5 Ga. Whether the data from these putative metasedimentary rocks reflect detrital zircon grains older than c. 2.7 Ga and a smear of metamorphic ages between two high-grade metamorphic events at *c.* 2.7 and *c.* 2.5 Ga, or a smear of detrital grains derived from protoliths older than 2.5 Ga followed by high grade metamorphism at *c.* 2.5 Ga, is unclear. An in situ SIMS Pb–Pb age of 2526 ± 8 Ma from a monazite included within garnet in an aluminous metasedimentary rock from north of Scourie is interpreted by Zhu et al. (1997) to date a second granulite facies metamorphic event.

**3. Field relations of the layered ultramafic–mafic bodies and metasedimentary rocks**

Notwithstanding that the large ultramafic–mafic bodies are bounded by steeply dipping amphibolite facies shear zones, several of the bodies preserve pristine granulite facies mineral assemblages in their core (O'Hara 1961, 1965; Johnson et al., 2012). While the igneous origin of these bodies is not disputed, whether the commonly observed mineralogical layering is a primary magmatic feature and whether apparent current and wedge cumulate mineral 'bedding' reflect magma chamber processes have been matters of vigorous debate (Bowes et al., 1964, 1966; O'Hara, 1965, 1966). Well exposed layered sequences of ultramafic and mafic rocks occur near Scourie, Drumbeg, Achiltibuie and Ben Strome, as well as in the southern part of the steeply dipping LSZ, in particular on Gorm Chnoc (Bowes et al., 1964; Davies, 1974; Sills et al., 1982; Fig. 2).

Although there are local complexities and repetition of rock types that could be either primary or due to post-emplacement deformation, the generalized sequence (Fig. 4a,b) comprises metamorphosed layered ultramafic rocks (hornblende-bearing metapyroxenites and metaperidotites mainly composed of assemblages of olivine, clinopyroxene, orthopyroxene, hornblende, spinel and magnetite) at or near the base overlain by medium- to coarse-grained hornblende-bearing two-pyroxene mafic rocks (mainly composed of assemblages of plagioclase, clinopyroxene, hornblende and orthopyroxene with or without garnet). In some instances the mafic rocks may be subdivided into a coarse-grained, plagioclase-deficient but garnet-rich lower unit overlain by a medium- to coarse-grained upper unit containing little or no garnet but a higher proportion of plagioclase. Where such a relationship exists, the change from one variant to the other is gradational. In some examples, felsic layers near the top of the sequence have been termed anorthosite and interpreted as primary, produced by fractionation of the mafic magmas (Bowes et al., 1964; Davies, 1974). In other cases, these felsic layers have been interpreted as intrusive (Weaver and Tarney, 1980), corresponding to crystallised melt derived from anatexis of the metabasic rocks (Johnson et al., 2012).

Individual ultramafic–mafic bodies commonly preserve only a portion of the succession described above, in many cases due to subsequent faulting/shearing. However, in all of the larger layered bodies mafic rocks are dominant. Although ultramafic rocks may constitute up to a third of some bodies by area (e.g. in the body near Drumbeg; Fig.1; Bowes et al., 1964), in many cases ultramafic rocks are absent.

Where exposed, brown gneisses commonly occur within synclinal cores of the larger ultramafic–mafic bodies at the highest structural levels, although similar lithologies may occur as highly strained units enclosed within the felsic orthogneisses. The most extensive exposures of brown gneiss occur in the southern part of the LSZ (Davies, 1974; Fig. 2), in the core of the Cnoc an t'Sidhean body SE of Stoer (Cartwright et al., 1985; Cartwright and Barnicoat 1986; Zirkler et al., 2012; Fig. 1) and around 1 km NNW of Scourie (Beach, 1974; Zhu et al., 1997; Fig. 1 and 2). The brown gneisses contain garnet, biotite and/or hornblende, plagioclase, quartz and accessory minerals, in which the proportion of mafic to felsic minerals varies widely. They range in composition from hornblende-rich metaluminous variants to peraluminous biotite-rich sillimanite- and kyanite-bearing gneisses that lack hornblende. In situ partial melting and two phases of garnet growth suggest the brown gneisses were metamorphosed to granulite facies then experienced extensive amphibolite facies (probably Inverian) retrogression (Zirkler et al., 2012).

Steeply-inclined shear zones at the margins of the ultramafic–mafic bodies in the southern part of the LSZ are characterised by amphibolite-facies mineral assemblages and a strong S- to SE-plunging stretching lineation which, in appropriate rocks, is defined by elongate garnet porphyroblasts, attesting to intense post-Badcallian deformation. In close proximity to the ultramafic–mafic bodies, the TTG gneisses are also strongly retrogressed, comprising assemblages including plagioclase, quartz, green hornblende, biotite and epidote.

## 4. Geochemistry

Major and trace element concentrations were determined for 29 metabasic rocks (from Johnson et al., 2012), 14 ultramafic rocks, 17 brown gneisses (from Zirkler et al., 2012 and new data; only 9 samples analysed for trace elements), 12 felsic sheets interpreted to have been derived from partial melting of the metabasic rocks (from Johnson et al., 2012), and 17 retrogressed (hornblende- and/or biotite-bearing) TTG gneisses collected from within 50 metres of a large ultramafic–mafic body. The metabasic rocks are subdivided into those that contain little or no garnet (n=14; hereafter garnet-poor metabasic rocks) and those that contain abundant garnet (n=15; hereafter garnet-rich metabasic rocks). Analytical procedures follow Johnson et al. (2012) and Zirkler et al. (2012). The full geochemical dataset is available in the Supplementary Data.

Included for comparison in the figures and discussion below are the compositions of (i) komatiites (n > 200) from greenstone belts within the Superior Province and North Atlantic craton using appropriate analyses from the GEOROC database (http://georoc.mpch-mainz.gwdg.de/); (ii) Archean (meta)basalts (n = 72) from greenstone belts from the Superior and North Atlantic cratons [hereafter SNAC basalts; data from Kerrich et al. (1999) – Mg- to Fe-tholeiitic basalts from the Superior Province; Polat (2009) – tholeiitic and transitional alkaline basalts from the Superior Province; Ordóñez-Calderón et al. (2011) – mafic amphibolites from SW Greenland interpreted as metamorphosed basalts produced in a subduction environment]; (iii) the major element compositions of 14 Archean non-arc basalts considered to represent near-primary partial melts of fertile mantle sample KR–4003 (Walther, 1998; Herzberg et al., 2010); (iv) the composition of mid ocean ridge basalt (MORB) according to Hofmann (1988) and Sun and McDonough (1989), the latter of which has a major element composition that is practically indistinguishable from the mean composition of 'ALL MORB' determined by Gale et al. (2013); and, (v) garnet–biotite gneisses from the Storø greenstone belt, SW Greenland (Ordóñez-Calderón et al., 2011) that are petrographically similar to the brown gneisses. Also shown are the mean compositions of olivine (ol) and clinopyroxene (cu) from a typical metamorphosed ultramafic rock (SC03) and clinopyroxene (cm) from a typical garnetiferous mafic rock (SC01) as measured by EPMA (Johnson and White, 2011; unpublished data). Both these samples are from near Scourie in the Assynt block (Fig. 1).

### *4.1. Major oxides*

Figure 5 shows the concentration of selected major oxides and $X_{\mathrm{Mg}}$ [molar MgO/(MgO/FeO)] plotted against MgO (wt%), on which the average compositions of all mafic rocks, metamorphosed ultramafic rocks and the Archean non-arc basalts are shown for reference. The metamorphosed ultramafic rocks contain 41–50 wt% $SiO_2$ and 32–19 wt% MgO, and have $X_{Mg}$ of 0.76–0.84. A linear trend is evident for most oxides that projects close to the mean composition of olivine in the ultramafic sample SC03 at its high MgO end and close to the average composition of the Archean non-arc basalts at its low MgO end. $SiO_2$, $TiO_2$, $Al_2O_3$, CaO, $Na_2O$ and MnO (not shown) are all negatively correlated against MgO (Fig. 5). The average composition of the ultramafic rocks is similar to the most MgO-rich of the Archean non-arc basalts, which together define a compositional trend for several oxides ($SiO_2$, $Al_2O_3$, FeO and CaO) when plotted against MgO that is considered to be a function of the temperature and degree of partial melting of the mantle, both of which increase with increasing MgO (e.g. Herzberg et al., 2010; Johnson et al., 2014).

All analysed mafic rocks are olivine normative (6–20 vol.%) except three garnet-poor samples that contain minor (<2.5 vol.%) normative quartz. Although there is considerable compositional spread and overlap, and few clear compositional trends, the variation diagrams show that the garnet-poor and garnet-rich metabasic rocks exhibit some compositional differences. In general, garnet-poor samples have higher $SiO_2$ and $Na_2O$ and lower FeO and $Al_2O_3$ contents compared to garnet-rich samples (Fig. 5; Johnson et al., 2012). A weak linear trend evident in the plot of MgO vs $Al_2O_3$, defined largely by the garnet-rich metabasic rocks, extends towards the average compositions of clinopyroxene at its low $Al_2O_3$, high MgO end. The overall compositional range of the mafic rocks is similar to the SNAC basalts, although several are relatively depleted in $SiO_2$, $Na_2O$, $TiO_2$ and $K_2O$ and slightly enriched in MgO, CaO and possibly FeO. The $X_{Mg}$ of the metabasic rocks varies widely from 0.34–0.74, similar to that recorded by the SNAC basalts. Compared to MORB, the average of all mafic rocks contains similar concentrations of MgO, CaO and $Al_2O_3$, but is moderately to strongly depleted in $Na_2O$, $TiO_2$ and $SiO_2$ and slightly enriched in $K_2O$.

The brown gneisses have major oxide compositions that are generally indistinguishable from those of the retrogressed TTG gneisses and felsic sheets, although some samples are relatively enriched in FeO and MnO (not shown) and depleted in $Na_2O$. The brown gneisses, TTG gneisses and felsic sheets together define a linear trend for many of the major oxides (excluding $TiO_2$) that broadly projects towards the average of the mafic rocks and MORB at higher MgO and lower $SiO_2$, although there is significant scatter in $Al_2O_3$, $Na_2O$ and $K_2O$.

Figure 6a shows the composition of the ultramafic and mafic rocks plotted on an AFM diagram (A = $Na_2O + K_2O$; F = total Fe expressed as FeO; M = MgO). Most have low total alkali contents and define a trend of strong enrichment in Fe that is characteristic of tholeiitic magmas. Although it is unclear which, if any, of the rocks are volcanic, Fig. 6b shows the compositions of the metabasic rocks and brown gneisses plotted on the total alkalis versus silica (TAS) diagram (Le Maitre et al., 2002). The mafic rocks generally lie within the basalt field, with four of the garnet-rich and one of the garnet-poor samples plotting within the picrobasalt field, and two of the garnet-poor samples within the basaltic andesite field. In the TAS diagram, the brown gneisses plot across a range of fields from basalt to rhyolite, with most plotting in the fields of andesite and dacite (Fig. 6b).

*4.2. Trace elements*

The primitive mantle normalised trace element compositions of the main rock types are shown in Fig. 7 in which elements are ordered from left to right by increasing compatibility in oceanic basalts (Hofmann, 1988). Data for the felsic sheets are given in Johnson et al. (2012).

The ultramafic rocks mostly have flat patterns for the more compatible trace elements with concentrations that are around 1–3 times primitive mantle values (Fig. 7a). All samples contain concentrations of Cs and Rb that are around an order of magnitude higher than primitive mantle; K and light rare earth element (LREE) contents are highly variable. A small negative Ti anomaly is evident and several samples have concentrations of Nb and Ta similar to, or below, primitive mantle values.

Relative to SNAC basalts and MORB (light and dark grey fields in Fig. 7c and d, respectively), almost all metabasic rocks (those with high $P_2O_5$ contents are excluded; Johnson et al., 2012) are weakly to strongly depleted in Hf, Zr and Ti, and several of the garnet-poor samples and many of the garnet-rich samples are moderately to strongly depleted in Th, U, Nb and Ta (Fig. 7b,c). All mafic rocks show highly variable LILE concentrations (Cs, Rb, Ba, K) that are elevated relative to MORB but similar to the range recorded by SNAC basalts (Fig. 7b,c).

The brown gneisses (Fig. 7d) have trace element compositions similar to the retrogressed TTG gneisses (Fig. 7e), although the former show greater variation in Hf and Zr, less variation in heavy rare earth element (HREE) contents and are marginally less depleted in Ti. Relative to petrographically similar garnet–biotite gneisses from the Storø greenstone belt, SW Greenland (Ordóñez-Calderón et al., 2011; grey field in Fig. 7d), a majority of brown gneiss samples are depleted in Cs, Rb, Th, U, Nb, Ta and Zr but enriched in Sr. Felsic sheets within the ultramafic–mafic bodies have trace element compositions similar to proximal TTG gneisses, although many show some relative depletion in Nb, Ta, Ti and Y (Johnson et al., 2012).

Figure 4c shows REE abundances normalised to CI chondrite of McDonough and Sun (1995), in which the plots are arranged in the simplified stratigraphic order described previously. Ultramafic rocks have REE abundances ≤ 10 times chondrite values (cf. Sills et al., 1982) and flat patterns in which $(La/Lu)_N$ = 1–2, except three samples with higher LREE concentrations and moderately fractionated patterns (Fig. 4c).

Garnet-rich mafic rocks have significantly lower LREE concentrations than garnet-poor variants (Fig. 4c). Several garnet-rich samples are LREE depleted [$(La/Sm)_N$ <1] with flat middle to heavy REE patterns, others have $(La/Lu)_N$ > 1 (Johnson et al., 2012). A small positive Eu anomaly (Eu/Eu* up to 1.5) occurs in three samples. In comparison, garnet-poor mafic rocks have a wider range of REE abundances. Although all samples have flat middle to heavy REE patterns, there are two compositional groups apparent, one with flat LREE patterns and another showing pronounced LREE enrichment [$(La/Sm)_N$ up to 3.5; Fig. 4c]. Both small positive and negative Eu anomalies occur (Eu/Eu* = 0.6–1.4), although the majority are negative (Johnson et al., 2012).

The retrogressed host TTG gneisses have steep REE patterns [mean $(La/Lu)_N$ of 41] and exhibit pronounced LREE enrichment with $(La/Sm)_N$ of 3–8. Most samples show a positive Eu anomaly in which the magnitude of Eu/Eu* (up to 2.8) is inversely correlated with overall REE abundance. The brown gneisses have moderately fractionated REE patterns [$(La/Lu)_N$ = 2–42] and a relative enrichment of LREE to HREE, in which $(La/Sm)_N$ = 2.5–6.3 and $(Gd/Lu)_N$ = 1.0–3.8. Samples exhibit small Eu anomalies that are both positive and negative (Eu/Eu* = 0.8–1.8). The concentration of HREE in the brown gneisses is similar to the metabasic rocks and, in general, significantly higher than in the TTG gneisses.

## 5. Discussion

Within the central region of the mainland Lewisian Complex, the rocks record evidence of polyphase deformation and at least three phases of granulite to amphibolite facies metamorphism, including partial melting of most rocks, during a tectono-metamorphic evolution spanning around a billion years. The field relationships and igneous, structural, metamorphic and geochemical (including isotopic) information preserved in the rocks reflect this complicated, long-lived high-temperature tectonic evolution. As a result, the early (pre-Badcallian to Badcallian) structural evolution is difficult or impossible to unravel and the compositional data as it pertains to the origin and early evolution of the rocks is ambiguous. Such a situation is not unique to the Lewisian Complex, but is a common feature of Archean high-grade grey gneiss terrains (e.g. West Greenland, Nutman et al., 2013, 2015), leading to inherent ambiguity in constraining the geodynamic regime responsible for the origin of these terrains.

### *5.1. The nature of the protoliths*

#### *5.1.1.Major oxide compositions*

Sills et al. (1982) proposed that the composition of the ultramafic and mafic rocks could be explained by fractionation via crystal settling of dominantly olivine and pyroxene from a high MgO ‘komatiitic’ mantle-derived (tholeiitic) melt, a conclusion supported by the whole rock major oxide data presented here. Plotted against MgO content, the metamorphosed ultramafic rocks define a broad trend between the average composition of olivine from a typical metamorphosed ultramafic rock and the average composition of Archean non-arc basalts (Fig. 5). The mafic rocks show considerable scatter for the major oxides. This likely reflects a complex combination of igneous processes (mainly olivine- and clinopyroxene-dominated fractional crystallisation of the primary magmas), and high-grade metamorphic processes (partial melting and melt loss from the mafic rocks, and possible contamination by TTG host rocks and melts derived therefrom; Johnson et al., 2012, 2013).

Notwithstanding, the average compositions of the metamorphosed ultramafic rocks, the mafic rocks and the Archean non-arc basalts define a broadly co-linear trend for all major oxides, except $SiO_2$ and $Na_2O$ (see below). This relationship suggests a possible genetic link between the ultramafic rocks, mafic rocks and a magma similar in composition to an average of the Archean non-arc basalts. On this basis we propose that the metamorphosed ultramafic rocks could represent the earliest cumulate material whereas the evolving melt could have fractionated to form the range of mafic compositions (cf. Sills et al., 1982).

Most ultramafic and mafic rocks contain brown (Ti-rich) hornblende interpreted to have been stable at the metamorphic peak (Johnson et al., 2012). This indicates that these rocks were hydrated prior to granulite facies metamorphism. Whether the primary magmas from which these rocks crystallised were hydrated, or whether the $H_2O$ was introduced subsequently, is uncertain. However, the observation that brown hornblende is apparently evenly distributed throughout the ultramafic–mafic rocks rather than developed only at the margins of the large ultramafic–mafic bodies and/or along planar structures that might record channelized fluid influx, suggests the primary magmas may have been hydrous and were derived from a hydrated mantle source.

The marked depletion in $TiO_2$ in the rocks relative to primitive mantle compositions (Fig. 7) likely reflects characteristics of the mantle source. However, the overall enrichment of the garnet-poor mafic rocks in $SiO_2$ and $Na_2O$ and depletion in $Al_2O_3$ relative to the garnet-rich samples may suggest that the latter comprise a higher proportion of the cumulate and retained less trapped melt than the former prior to solidification. This interpretation is consistent with the simplified stratigraphic sequence shown in Fig. 4a. Although we follow Sills et al. (1982) and Johnson et al. (2012) in interpreting most of the mafic rocks as metamorphosed intrusive rocks (i.e. metagabbros), is it possible that some of the garnet-poor mafic rocks, particularly those occurring near the structural tops of the large ultramafic–mafic bodies, were extrusive (i.e. metabasalt).

Concentrations of $SiO_2$, $Na_2O$ and $K_2O$ in the mafic rocks are on average depleted relative to SNAC basalts, as illustrated in Fig. 8. This feature conforms to a general model of partial melting of amphibolite whereby the mafic rocks are residual after extraction of melt, in which melt compositions are consistent with the felsic sheets (Johnson et al., 2012; Fig. 5). Depletion of $SiO_2$ and $Na_2O$ by melting of the metabasic rocks explains the nonconformity of these major oxides with the fractionation trend discussed above.

*5.1.2. Trace element compositions*

During the past forty years geochemical methods have been developed to enable discrimination among tectonically defined magma types for volcanic rocks, in particular basalts (e.g. Pearce and Cann, 1973; Pearce and Peate, 1995; Pearce, 2008). Such discrimination has proven particularly useful where the magma source cannot be unambiguously deduced using other methods, for example in the case of ophiolites (Pearce, 2008, 2014b). However, the ability to correctly discriminate samples from mid-ocean ridges, island arcs and ocean islands using binary and ternary diagrams has been assessed as no better than 60% (Snow, 2006), and the use of these diagrams at all in discrimination of magma type has been challenged (Li et al., 2015). This calls into question whether such diagrams should be used in assessing the tectonic setting of Archean greenstones (Pearce, 2008; Condie, 2015).

In this study it is unclear which, if any, of the samples might have had the volcanic protoliths that are generally required for geochemical discrimination of magma type. Furthermore, the extent to which trace element data may be used to elucidate tectonic environments in rocks that have undergone strong modification by magmatic and metamorphic fractionation, as well as probable contamination with their host rocks, is questionable (Pearce, 2008, 2014a; Rollinson and Gravestock, 2012). Although many trace elements may be considered immobile during high-temperature subsolidus metamorphism and hydrothermal alteration, most have mineral/melt distribution coefficients that are far from unity, leading to significant modification of trace element compositions as a result of crystal settling and/or partial melting and melt loss (Fig. 8). Notwithstanding, the trace element compositions may be useful in interpreting some aspects of source characteristics (Condie, 2015).

The brown gneisses show significant depletion in most LILE compared to petrographically similar garnet–biotite gneisses from SW Greenland (Ordóñez-Calderón et al., 2011; Fig. 7a), consistent with partial melting and melt loss (Cartwright and Barnicoat, 1987; Zirkler et al., 2012). The trace element composition of the brown gneisses is broadly similar to that of the TTG gneisses (Fig. 7), except for the HREE contents, which are similar to the mafic rocks but mostly higher than in the TTG gneisses (Fig. 4c). This indicates that the brown gneisses cannot have been formed solely from the TTG gneisses.

For the garnet–biotite gneisses and associated quartz-rich rocks from southern West Greenland, the petrogenetic interpretation preferred by Ordóñez-Calderón et al. (2011) is that some represent metamorphosed altered basaltic rocks (greenstones) whereas the bulk are metamorphosed siliciclastic rocks derived by erosion of a mixture of felsic and mafic igneous rocks. However, these authors acknowledge ambiguity in their interpretation. The brown gneisses in the central region of the Lewisian complex are similarly enigmatic. Their protoliths could conceivably have been: (i) sedimentary rocks derived by erosion of both the TTG-dominated crust and associated ultramafic–mafic complexes prior to the granulite facies metamorphism; (ii) erupted (volcanic) equivalents of the mafic to felsic plutonic rocks; (iii) orthogneisses metasomatised during the prograde granulite facies metamorphism; or (iv) one or more combinations of the origins suggested in (i) to (iii). Based on the general spatial and stratigraphic distribution of the brown gneisses (Fig. 2) and the rounded nature of the zircons (Zirkler et al., 2012; Goodenough et al., 2013), the interpretation preferred here is that most of the brown gneisses represent metamorphosed sedimentary or volcano-sedimentary rocks.

Accepting the caveats discussed above concerning binary discrimination diagrams, the composition of the brown gneisses is compared with similar rocks from southern West Greenland, and the mafic rocks (which may or may not approximate liquid compositions) with the SNAC basalts on three popular discrimination diagrams (Fig. 9). On the Ti/Y vs Nb/Y diagram the brown gneisses plot in fields ranging from basalt to rhyolite/dacite, similar to the garnet–biotite gneisses from Greenland (Fig. 9a), whereas most of the mafic rocks plot within the basalt field, with the remainder plotting within the basaltic andesite/andesite field at higher Ti. Excluding those non-basaltic samples (i.e. those with $SiO_2 > 60$ wt%), on the Th/Yb vs Nb/Yb diagram (Fig. 9b) the brown gneisses are scattered, with three of the four samples plotting close to or below the MORB–ocean island basalt (OIB) array. By contrast, the Greenland samples plot in the field of continental arc rocks above the MORB–OIB array at high Nb/Yb (Pearce, 2008). The mafic rocks show no coherent trend in Fig. 9b; several samples plot below the MORB–OIB array, consistent with partial melting and melt loss. On the Nb/Y vs $TiO_2$/Yb diagram (Fig. 9c) the four low-silica brown gneisses lie in or below the MORB array, with three plotting close to the composition of E–MORB, although this proxy is not considered effective for fingerprinting Archean tectonic settings (Pearce 2008). Most of the mafic rocks also plot in the MORB array and many plot close to the composition of N–MORB.

A pronounced depletion in Nb, Ta and Ti is a characteristic geochemical signature of rocks from the Lewisian Complex (Fowler, 1986; Rollinson, 1996) and is seen in all samples in this study (Fig. 7). Several of the ultramafic rocks have concentrations of Nb and Ta that are lower than primitive mantle values (Fig. 7a), the mafic rocks are depleted relative to

SNAC basalts and MORB (Fig. 7b,c; Fig. 8; Johnson et al., 2012), the brown gneisses are depleted relative to similar rocks in Greenland (Fig. 7d) and the proximal TTG gneisses (Fig. 7e; discussed in detail below). This 'arc-like' signature may be interpreted to reflect the presence of rutile in the source rocks at depth, a feature that is commonly invoked to indicate formation in a subduction environment (e.g. Moyen, 2011).

Central region TTG gneisses have the high $SiO_2$, Na/K, Sr/Y and depleted HREE signatures that characterise most sodic Archean TTGs worldwide, consistent with an interpretation that most TTGs equilibrated with a garnet- and clinopyroxene-bearing (with or without hornblende) residue that lacked plagioclase (Moyen, 2011). Moreover, TTG gneisses from the central region show a pronounced depletion in Ta, Nb and Ti relative to an average sodic TTG composition (Johnson et al., 2013, fig. 2), suggesting their source rocks also contained rutile. A common hypothesis is the TTG gneisses formed by partial melting of garnet- and rutile-bearing amphibolites or eclogites in a subducting slab (e.g. Drummand and Defant, 1990; Martin, 1999; Rapp et al., 2003). However, the presence of garnet- and rutile-bearing residual source rocks that exhausted plagioclase does not necessarily mean that those source rocks were eclogites or that the source rocks were stable at eclogite facies pressures (e.g. Johnson et al., 2014). Both experiments (Qian and Hermann, 2013; Zhang et al., 2013) and phase equilibria modelling (Johnson et al., 2014) show that suitable garnet- and rutile-bearing residues can be produced at pressures of 1.5 GPa or less. In addition, geochemical and experimental data suggest that most TTGs, including those from the Lewisian Complex, were derived from a LILE-enriched source similar to oceanic plateau basalts, and are unlikely to have been derived from anatexis of MORB in a subduction zone setting (Martin et al., 2014).

Negative anomalies in Nb, Ta and Ti as well as an enrichment in Th, LREE and other LILE are recorded in younger (Palaeoproterozoic) rocks of the Scourie Dyke swarm and mantle xenoliths that sample the sub-continental mantle lithosphere underlying the Lewisian Complex (Hughes et al., 2014). Trace element modelling led Hughes and co-workers to conclude that the sub-continental mantle lithosphere was metasomatised by devolatilisation of a subducting slab during the Archean and/or had interacted with carbonatitic melts. Although subduction is one way of getting hydrated material into the mantle, it is not the only plausible mechanism. Bédard (2006) suggested that TTG magmas may be generated at the base of thick plateau-like units of hydrated basaltic crust. In his model, the dense garnet- and hornblende-bearing residues delaminated, refertilising the sub-continental mantle lithosphere and triggering additional melting (see also Bédard et al., 2003, 2013). Geodynamic models that consider higher mantle temperatures appropriate to the Archean and incorporate calculated phase equilibria and experimentally determined melting relations have demonstrated the plausibility of this alternative mechanism of mantle refertilisation (Johnson et al., 2014; Sizova et al., 2015). In summary, similar to other regions, the trace element composition of rocks from the central region of the Lewisian Complex does not allow unambiguous discrimination of the tectonic setting in which the rocks formed (cf. Pearce, 2014a).

### *5.2. Field and metamorphic evidence*

Large kilometre- to decametre-scale layered ultramafic–mafic bodies within the central region of the Lewisian Complex are distinct from smaller ultramafic and mafic sheet-like and podiform bodies that are ubiquitous at outcrop scale throughout the central region. The difference is not just in scale (the layered bodies are larger by an order of magnitude or more), but also in the fact that many of the metabasic rocks in the layered bodies contain abundant garnet, whereas the smaller sheet-like bodies do not. Nonetheless, the large ultramafic–mafic bodies could be genetically related to these smaller bodies.

Based on field evidence from Badcall (Fig. 1), Rollinson and Windley (1980) suggested that the TTG gneisses intruded, and therefore post-dated, the layered ultramafic–mafic bodies (their figure 1), an interpretation followed by Rollinson and Gravestock (2012). During the course of this work we have found no convincing evidence in the field, at Badcall or elsewhere, to support this interpretation (although the mafic rocks are commonly cross-cut by bodies of tonalite–trondhjemite derived from partial melting of the mafic rocks and TTG gneisses; Johnson et al., 2010). In addition, this relative age relationship contradicts the isotopic age data, much of which suggests that the TTG gneisses are older than the mafic–ultramafic rocks (Whitehouse, 1989; Cohen et al., 1991; Friend and Kinny, 1995; Whitehouse et al., 1996; Kinny and Friend, 1997; Burton et al., 2000; Fig. 3).

The large layered ultramafic–mafic bodies are bounded by steeply dipping shear zones. Furthermore, some of these bodies are spatially associated with brown gneisses of probable supracrustal origin. The folded and disrupted belt of layered ultramafic–mafic bodies and brown gneisses in the south of the LSZ shows a broadly symmetrical distribution of rock types (Fig. 2). If this belt represents lateral accretion due to closure of an ocean basin via asymmetric (one-sided) subduction, then the metamorphosed equivalents of other lithologies typically associated with active margins (e.g. ophiolites, mélanges/olistostromes, cherts, banded iron formations (BIF), black shales, carbonate rocks, etc.), are notably lacking in the central region. Although such lithological associations diagnostic of subduction–accretion do occur in the mainland Lewisian Complex, forming the Loch Maree Group within the southern region (Park et al., 2001), these protoliths are significantly younger (c. 2.0 Ga; O'Nions et al., 1983; Whitehouse et al. 1997) than those in the central region, and record Paleoproterozic, not Archean, processes (Park et al., 2001; Mason, 2015).

Assuming the brown gneisses represent supracrustal rocks, the spatial relationship between the brown gneisses and several ultramafic–mafic bodies requires burial of these lithologies from the near surface to depths exceeding 25 km prior to or during granulite facies metamorphism. Folding of the ultramafic–mafic belts and associated supracrustal rocks is considered by Davies (1976) to have occurred during the Archean prior to the peak of Badcallian metamorphism. Thus, the geometry of both the belt of ultramafic–mafic bodies and supracrustal rocks in the southern LSZ, as well as more isolated ultramafic–mafic bodies, could be interpreted in terms of pre- to syn-Badcallian gravity-driven sinking (sagduction) of the dense ultramafic–mafic bodies (and structurally-overlying supracrustal rocks) into the underlying less dense and less viscous partially molten TTG gneisses (cf. Anhaeusser, 1975; Brun, 1980; Brun et al., 1981; Ramsay, 1989; Bouhallier et al., 1995; Kisters & Anhaeusser, 1995; Chardon et al., 1996, 1998; Collins et al., 1998; Bremond d'Ars et al., 1999; Marshak, 1999; Wellman, 2000; Sandiford et al., 2004; Van Kranendonk et al., 2004, 2014; Parmenter et al., 2006; Robin and Bailey 2009; Thebaud and Rey 2013; François et al., 2014; Sizova et al., 2015).

Based on mineral equilibria modelling, there is no evidence that the ultramafic–mafic rocks reached pressures significantly higher than the inferred Badcallian metamorphic peak (Johnson and White, 2011). The implied clockwise $P$–$T$ path, in which peak $T$ and $P$ coincide (Johnson & White, 2011, fig. 5b), is similar to those modelled for Archean sagduction (Francois et al., 2014), the results of which suggest the process is rapid and occurs within a few million years. The apparent thermal gradient of ~925 ºC/GPa lies within the range for Precambrian granulite–ultrahigh temperature metamorphism (750–1500 ºC/GPa) but well above that for Precambrian eclogite–high pressure granulite metamorphism (350–750 ºC/GPa) that has been interpreted to record the start of Archean subduction (Brown, 2014). Furthermore, Phanerozoic subduction–accretion is associated with more hairpin-like clockwise *P–T* paths in which the pressure peak coincided with or preceded the temperature peak (e.g. Liou et al, 2014). There is no evidence for regional blueschist or eclogite facies metamorphism in the central region that is a signature of late Neoproterozoic and Phanerozoic subduction. If it is confirmed that fragments of garnet pyroxenite in the ultramafic–mafic bodies reached eclogite facies, as reported by Sajeev et al. (2013), an origin as entrained deep-seated remnants of delaminating lower crust is a plausible explanation (Sizova et al., 2015).

Although primary (early) structural relationships have been destroyed by the intense polyphase ductile deformation, some of the smaller metre- to centimetre-scale ultramafic and mafic sheet-like bodies that are ubiquitous within the central region could represent disrupted dykes through which the original greenstone belt magmas were supplied from depth. Also, the geochemistry of these smaller bodies is likely to reflect interaction with the suprasolidus (melt-bearing) host TTG gneisses, as suggested by the variable REE chemistry of clinopyroxene from ultramafic rocks preserved at different scales (Rollinson and Gravestock, 2012).

Sinking of the large layered ultramafic–mafic bodies and associated supracrustal rocks during the Archean prior to or synchronous with Badcallian granulite facies metamorphism would have given rise to structures with steeply dipping foliations and lineations at their margins (Collins et al., 1998; Marshak, 1999; Van Kranendonk et al., 2004; Parmenter et al., 2006; Lin and Beakhouse, 2013; Thébaud and Rey, 2013), perhaps consistent with the initial (pre- to syn-Badcallian) development of the shear zones that occur at the margins of these bodies. However, subsequently these structures would have acted as strong foci for deformation and fluid flow, in agreement with the strong localisation of strain and retrogression during the subsequent Inverian and Laxfordian events, which caused extensive overprinting of pre- to syn-granulite facies deformation and mineral assemblages.

A strong S- to SE-plunging stretching lineation defined by garnet is common at the margins of the large ultramafic–mafic bodies, attesting to intense post-Badcallian deformation of these bodies. Despite the fact that unambiguous evidence is absent due to successive overprinting deformations, the shear zones spatially associated with the ultramafic–mafic bodies may represent early (Badcallian) structures that were subsequently reactivated by Inverian and Laxfordian deformation.

Although the fundamental driving force for sagduction of greenstone belts is the negative buoyancy of the denser ultramafic and mafic rocks ($\rho > 3.0$ gcm$^{-3}$) relative to underlying felsic orthogneisses ($\rho \sim 2.7$ gcm$^{-3}$), it is thermal weakening of the basement and a low viscosity in the immediately underlying mantle that control the process (Sandiford et al., 2004; Thebaud and Rey 2013; Johnson et al., 2014). The dynamic requirements for sagduction were evidently met in many greenstone belts (Anhaeusser 1975; Brun 1980; Brun et al., 1981; Bouhallier et al., 1995; Chardon et al., 1996, 1998; Collins et al., 1998; Parmenter et al., 2006; Robin and Bailey 2009; Wellman, 2000) and sagduction plausibly could have occurred in the central region of the Lewisian Complex, particularly as the basement rocks at depth were at temperatures in excess of 900 °C and partially molten (Johnson et al., 2013).

The ultramafic–mafic bodies could conceivably represent the metamorphosed equivalents of: accreted oceanic crust, lower crustal underplates, a single disrupted large layered intrusion emplaced into felsic crust, multiple layered intrusions of a similar age, multiple layered intrusions of variable age, differentiated intrusions near the base of a greenstone belt, or interlayered komatiitic and basaltic lava flows near the base of a greenstone belt. The brown gneisses may represent (volcano) sedimentary rocks from higher crustal levels. If the rocks do represent the sunken remnants of dense upper crust, at some point the downward motion of the greenstone belts was arrested. Why would this have happened?

The ultramafic–mafic bodies, metasedimentary rocks and host TTG gneisses record similar peak *T* and *P* conditions (Johnson and White 2011; Zirkler et al., 2012; Johnson et al., 2013), which implies they were present together in the deep crust close to the Badcallian metamorphic peak. One possible explanation for the arrested downward flow of the greenstones is stiffening of the crust at depth. If prograde melt production and drainage from the fertile TTGs ceased during sagduction of the greenstones as the metamorphic peak was approached and as heat flow declined, the residual TTG crust could have become significantly more viscous halting the sinking greenstones.

The dynamic plausibility of these processes requires evaluation using 2D and 3D geodynamic modelling. However, a recent study by Sizova et al. (2015) modelling Eoarchean–Mesoarchean geodynamics (at appropriate mantle temperatures) makes predictions that can explain the variety and complexity of the Archean geological record. These include formation of a pristine granite–greenstone-like crust with dome-and-keel geometry formed over delaminating–upwelling mantle, followed by the development of reworked (accreted) crust that is subjected to both strong horizontal shortening and vertical tectonics processes, which are terminated by short-lived subduction events. These non-uniformitarian models predict the formation of voluminous TTG-like magmas and ultimately produce discrete, shear-zone bounded crustal terranes that resemble the architecture of the Archean rocks within mainland Lewisian Complex.

*5.3. Future work*

Like other areas of Archean crust, unravelling the complexities recorded in the rocks of the Lewisian Complex to reveal their geodynamic evolution is difficult, not least because, despite a large volume of data, the geochemical and geochronological data are ambiguous. Finding some consensus on the absolute timing of 'events' may lie in analysing Sm–Nd and Lu–Hf isotopic composition of garnet and/or U–Pb analysis of zircon/baddeleyite within the mafic rocks. Resolving whether the various crustal blocks are disrupted then reassembled fragments of a single lithosphere unit or are exotic terranes may be resolved using Hf (and other) isotopic measurements of accessory minerals; the acquisition of such data is becoming increasingly faster and cost-effective. In addition, a detailed knowledge of the spatial distribution of Badcallian metamorphic conditions may inform the nature of the proposed terrane boundaries and the potential presence (or otherwise) of belts of rocks recording both higher and lower than average apparent thermal gradients that are a signature of subduction. This requires phase equilibria modelling of tens or hundreds of samples. More detailed mapping of the ultramafic–mafic bodies, brown gneisses and host rocks may provide some information on their early (pre- to syn-Badcallian kinematic history), although subsequent deformation may have destroyed this evidence throughout the Lewisian Complex.

## 6. Conclusions

The field evidence relating to the large ultramafic–mafic bodies, in particular as it relates to the early structural evolution, has been overprinted by subsequent events and is equivocal. The composition of the rocks is highly variable, probably as a consequence of magmatic differentiation in layered intrusive complexes, subsequent melting during ultrahigh-temperature metamorphism and interaction with neighbouring rocks and partial melts derived therefrom. As a result the geochemical characteristics are not clearly diagnostic of magmatic process or tectonic setting. The 'arc-like' signature exhibited by many Archean rocks is not unique to a subduction–accretion environment; there are other mechanisms of enriching mantle source rocks that are perhaps more plausible at the higher temperatures that would have characterised the Archean. Although a subduction origin is possible, we suggest that the layered kilometre- to decametre-scale ultramafic–mafic bodies and associated supracrustal rocks might be the remnants of greenstone belts that sank into partially molten TTG-dominated crust. Whether similar ultramafic–mafic complexes in other high-grade gneiss terrains represent evidence of subduction or were intracratonic should be re-evaluated on a case-by-case basis. However, the possibility that Archean cratonic fragments, which commonly comprise a collage of discrete terranes, could have been produced in a non-plate tectonic scenario is becoming increasingly hard to dismiss (Bédard et al., 2013; Johnson et al, 2014; Bédard and Harris, 2014; Sizova et al., 2015; cf. Polat et al., 2015).

## Acknowledgements

We thank Jean Bédard, Tim Ivanic, John Percival and anonymous for their reviews and John Wheeler for comments on an earlier version of the manuscript. KG publishes with the permission of the Executive Director of the British Geological Survey.

## References

Anhaeusser, C.R., 1975. Precambrian tectonic environments. Annual Review of Earth and Planetary Sciences, 3, 31–53.

Anhaeusser, C.R., 2001. The anatomy of an extrusive-intrusive Archean mafic-ultramafic sequence: the Nelshoogte schist belt and Stolzburg Layered ultramafic complex, Barberton greenstone belt, South Africa. South African Journal of Geology, 104, 167–204.

Anhaeusser, C.R., 2014. Archean greenstone belts and associated granitic rocks – A review. Journal of African Earth Sciences, 100, 684–732.

Ashwal, L.D., Tucker, R.D., Zinner, E.K., 1999. Slow cooling of deep crustal granulites and Pb-loss in zircon. Geochimica et Cosmochimica Acta, 63, 2839–2851.

Barnicoat, A.C., 1983. Metamorphism of the Scourian Complex, NW Scotland, Journal of Metamorphic Geology, 1, 163–182.

Beach, A., 1973. The mineralogy of high temperature shear zones at Scourie, NW Scotland. Journal of Petrology, 14, 231–248.

Beach, A., 1974. The measurement and significance of displacements on Laxfordian Shear Zones, North-West Scotland. Proceedings of the Geologists' Association, 85, 13–21.

Beach, A., 1976. The interrelations of fluid transport, deformation, geochemistry and heat flow in early Proterozoic shear zones in the Lewisian complex. Philosophical Transactions of the Royal Society of London A, 280, 569–604.

Beach, A., 1980. Retrogressive metamorphic processes in shear zones with special reference to the Lewisian complex. Journal of Structural Geology, 2, 257–263.

Beach, A., Fyfe, W.S., 1972. Fluid transport and shear zones at Scourie, Sutherland – evidence of overthrusting. Contributions to Mineralogy and Petrology, 36, 175–180.

Beach, A., Coward, M.P., Graham, R.H., 1974. An interpretation of the structural evolution of the Laxford Front, north west Scotland. Scottish Journal of Geology, 9, 297–308.

Bédard, J.H., 2006. A catalytic delamination-driven model for coupled genesis of Archean crust and sub-continental lithospheric mantle. Geochimica et Cosmochimica Acta, 70, 1188–1214.

Bédard, J. H., Brouillette, P., Madore, L., & Berclaz, A., 2003. Archean cratonization and deformation in the northern Superior Province, Canada: an evaluation of plate tectonic versus vertical tectonic models. Precambrian Research, 127, 61-87.

Bédard, J. H., & Harris, L. B., 2014. Neoarchean disaggregation and reassembly of the Superior craton. Geology, 42, 951–954.

Bédard, J.H., Harris, L.B., Thurston, P.C., 2013. The hunting of the snArc. Precambrian Research, 229, 20–48.

Blewett, R. S., 2002. Archean tectonic processes: a case for horizontal shortening in the North Pilbara Granite-Greenstone Terrane, Western Australia. Precambrian Research, 113, 87–120.

Bouhallier, H., Chardon, D., Choukroune, P., 1995. Strain patterns in Archean dome-and-basin structures – the Dharwar craton (Karnataka, south India). Earth and Planetary Science Letters, 135, 57–75.

Bowes, D.R., Wright, A.E., Park, R.G., 1964. Layered intrusive rocks in the Lewisian of the North-West Highlands of Scotland. Quarterly Journal of the Geological Society, 120, 153–192.

Bowes, D.R., Wright, A.E., Park, R.G., 1966. Correspondence. Origin of ultrabasic and basic masses in the Lewisian. Geological Magazine, 103, 280–283.

Bremond d'Ars, J.D., Lecuyer, C., Reynard, B., 1999. Hydrothermalism and diapirism in the Archean: gravitational instability constraints. Tectonophysics, 304, 29–39.

Brown, M., 2014. The contribution of metamorphic petrology to understanding lithosphere evolution and geodynamics. Geoscience Frontiers, 5, 553-569.

Brown, M., 2015. Paleo- to Mesoarchean polymetamorphism in the Barberton Granite-Greenstone Belt, South Africa: Constraints from U-Pb monazite and Lu-Hf garnet geochronology on the tectonic processes that shaped the belt: Discussion. Geological Society of America Bulletin, first published on April 30, 2015, doi:10.1130/B31198.1.

Brun, J.P., 1980. The cluster-ridge pattern of mantled gneiss domes in eastern Finland: evidence for large-scale gravitational instability in the Proterozoic crust. Earth and Planetary Science Letters, 44, 441-449.

Brun, J.P., Gapais, D., Le Theoff, B., 1981. The mantled gneiss domes of Kuopio (Finland): interfering diapirs. Tectonophysics, 74, 283–304.

Burton, K.W., Capmas, F., Birck, J-L, Allègre, C.J., Cohen, A.S., 2000. Resolving crystallisation ages of Archean mafic–ultramafic rocks using the Re–Os isotope system. Earth and Planetary Science Letters, 179, 453–467.

Cartwright, I., Barnicoat, A.C., 1986. The generation of quartz-normative melts and corundum-bearing restites by crustal anatexis: petrogenetic modelling based on an example from the Lewisian of North-West Scotland, Journal of Metamorphic Geology, 4, 79–99.

Cartwright, I., Barnicoat, A.C., 1987. Petrology of Scourian supracrustal rocks and orthogneisses from Stoer, NW Scotland: implications for the geological evolution of the Lewisian complex. In: Park, R. G., Tarney, J. (eds) Evolution of the Lewisian and Comparable Precambrian High Grade Terrains. Geological Society, London, Special Publications, 27, 93–107.

Cartwright, I., Fitches, W.R., O'Hara, M.J., Barnicoat, A.C., O'Hara, S., 1985. Archean supracrustal rocks from the Lewisian near Stoer, Sutherland. Scottish Journal of Geology, 21, 187–196.

Chardon, D., Choukroune, P., Jayananda, M., 1996. Strain patterns, décollement and incipient sagducted greenstone terrains in the Archean Dharwar craton (south India). Journal of Structural Geology, 18, 991–1004.

Chardon, D., Choukroune, P., Jayananda, M., 1998. Sinking of the Dharwar Basin (South India): implications for Archean tectonics. Precambrian Research, 91, 15–39.

Cohen, A.S., ONions, R.K., OHara, M.J., 1991. Chronology and mechanism of depletion in Lewisian granulites. Contributions to Mineralogy and Petrology, 106, 142–153.

Collins, W.J., Van Kranendonk, M.J., Teyssier, C., 1998. Partial convective overturn of Archean crust in the east Pilbara Craton, Western Australia: driving mechanisms and tectonic implications. Journal of Structural Geology, 20, 1,405–1,424.

Condie, K., 2015. Changing tectonic settings through time: Indiscriminate use of geochemical discriminant diagrams. Precambrian Research, 266, 587–591.

Corfu, F., Heaman, L.M., Rogers, G., 1994. Polymetamorphic evolution of the Lewisian complex, NW Scotland, as recorded by U-Pb isotopic compositions of zircon, titanite and rutile. Contributions to Mineralogy and Petrology, 117, 215–228.

Corfu, F., 2007. Comment to paper: Timing of magmatism and metamorphism in the Gruinard Bay area of the Lewisian gneiss complex: comparison with the Assynt Terrane and implications for terrane accretion by G.J. Love, P.D. Kinny and C.R.L. Friend (Contr Mineral Petrol (2004) 146:620–636). Contributions to Mineralogy and Petrology, 153, 483–488.

Coward, M.P., 1984. Major shear zones in the Precambrian crust; examples from NW Scotland and southern Africa and their significance. In: Kröner, A., Greiling, R. (eds) Precambrian Tectonics Illustrated. Stuttgart, Germany, E. Schweizerbart'sche Verlagsbuchhandlung, 207–235.

Coward, M.P., 1990. Shear zones at the Laxford Front, NW Scotland and their significance in the interpretation of lower crustal structure. Journal of the Geological Society, London, 147, 279–286.

Coward, M.P., Park, R.G., 1987. The role of mid-crustal shear zones in the Early Proterozoic evolution of the Lewisian. In: Park, R. G. and Tarney, J. (eds) Evolution of the Lewisian and Comparable Precambrian High Grade Terrains. Geological Society, London, Special Publications, 27, 127–138.

Crowley, Q.G., Key, R., Noble, S.R., 2015. High-precision U–Pb dating of complex zircon from the Lewisian Gneiss Complex of Scotland using an incremental CA-ID-TIMS approach. Gondwana Research, 27, 1381–1391.

Cutts, K.A., Stevens, G., Kisters, A., 2015. Reply to "Paleo- to Mesoarchean polymetamorphism in the Barberton granite-greenstone belt, South Africa: Constraints from U-Pb monazite and Lu-Hf garnet geochronology on the tectonic processes that shaped the belt: Discussion" by M. Brown. Geological Society of America Bulletin, first published on April 30, 2015, doi:10.1130/B31304.1.

Davies, F.B., 1974. A layered basic complex in the Lewisian, south of Loch Laxford, Sutherland. Journal of the Geological Society, London, 130, 279–284.

Davies, F.B., 1976. Early Scourian structures in the Scourie-Laxford region and theirbearing on the evolution of the Laxford Front. Journal of the Geological Society, London, 132, 543–554.

Davies, J.H.F.L., Heaman, L.M., 2014. New U–Pb baddeleyite and zircon ages for the Scourie dyke swarm: A long-lived large igneous province with implications for the Paleoproterozoic evolution of NW Scotland. Precambrian Research, 249, 180–198.

De Wit, M.J., Ashwal, L.D., 1997. Greenstone Belts. Oxford, Clarendon Press, ??? pp.

Drummond, M. S., & Defant, M. J., 1990. A model for trondhjemite–tonalite–dacite genesis and crustal growth via slab melting: Archean to modern comparisons. Journal of Geophysical Research: Solid Earth, 95(B13), 21503–21521.

Evans, C. R., 1965. Geochronology of the Lewisian basement near Lochinver, Sutherland. Nature, 207, 54–55.

Evans, C.R., Lambert, R.S.J., 1974. The Lewisian of Lochinver, Sutherland; the type area for the Inverian metamorphism. Journal of the Geological Society, 130, 125–150.

Fowler, M.B., 1986. Large-ion lithophile element characteristics of an amphibolite facies to granulite facies transition at Gruinard Bay, North-west Scotland. Journal of Metamorphic Geology, 4. 345–359.

François, C., Phillippot, P., Rey, P., Rubatto, D., 2014. Burial and exhumation during Archean sagduction in the East Pilbara Granite-Greenstone Terrane. Earth and Planetary Science Letters, 396, 235–251.

Friend, C.R.L., Kinny, P.D., 1995. New evidence for protolith ages of Lewisian granulites, northwest Scotland. Geology, 23, 1027–1030.

Friend, C.R.L., Kinny, P.D., 2001. A reappraisal of the Lewisian Gniess Complex: geochronological evidence for its tectonic assembly from disparate terrances in the Proterozoic. Contributions to Mineralogy and Petrology, 142. 198–218.

Gale, A., Dalton, C.A., Langmuir, C.H., Su, Y., Schilling, J-G., 2013. The mean composition of ocean ridge basalts. Geochemistry, Geophysics, Geosystems, 14, 489–518.

Gapais, D., Jaguin, J., Cagnard, F., Boulvais, P., 2014. Pop-down tectonics, fluid channelling and ore deposits within ancient hot orogens. Tectonophysics, 618, 102–106.

Goodenough, K.M., Crowley, Q.G., Krabbendam, M., Parry, S.F., 2013. New U–Pb constraints for the Laxford Shear Zone, NW Scotland: Evidence for tectono-magmatic processes associated with the formation of a Paleoproterozoic supercontinent. Precambrian Research, 233, 1–19.

Goodenough, K.M., Park, R.G., Krabbendam, M., Myers, J., Wheeler, J., Loughlin, S.C., Crowley, Q.G., Friend, C.R.L., Beach, A., Kinny, P.D., Graham, R.H., 2010. The Laxford Shear Zone: an end-Archean terrane boundary? In: Law, R., Butler, R.W.H., Holdsworth, R.E., Krabbendam, M., Strachan, R. (eds) Continental Tectonics and Mountain Building: The Legacy of Peach and Horne. Geological Society, London, Special Publications, 335, 103–120.

Goodwin, A.M., 1991, Precambrian Geology, Academic Press, London, 666 pp.

Goodwin, Smith, 1980. Chemical discontinuities in Archean volcanic terrains and the development of Archean crust. Precambrian Research, 10, 301–311.

Hamilton, P.J., Evensen, N.M., ONions, R.K., Tarney, J., 1979. Sm-Nd systematics of Lewisian gneisses: implications for the origin of granulites. Nature, 277, 25–28.

Herzberg, C., Condie, K., Korenaga, J., 2010. Thermal history of the Earth and its petrological expression. Earth and Planetary Science Letters, 292, 79–88.

Hofmann, A. W., 1988. Chemical differentiation of the Earth: the relationship between mantle, continental crust, and oceanic crust. Earth and Planetary Science Letters, 90, 297—314.

Horie, K., Nutman, A.P., Friend, C.R.L., Hidaka, H., 2010. The complex age of orthogneiss protoliths exemplified by the EoArchean Itsaq Gneiss Complex (Greenland): SHRIMP and old rocks. Precambrian Research, 183, 25–43.

Hughes, H.S.R., McDonald, I, Goodenough, K.M., Ciborowski, T.J.R., Kerr, A.C., Davies, J.H.F.L., Selby, D., 2014. Enriched lithospheric mantle keel below the Scottish margin of the North Atlantic Craton: Evidence from the Palaeoproterozoic Scourie Dyke Swarm and mantle xenoliths. Precambrian Research, 250, 97–126.

Irvine, A.J., Baragar, W.R.A., 1971. A guide to the chemical classification of the common volcanic rocks. Canadian Journal of Earth Sciences, 8, 523–548.

Jenner, F. E., Bennett, V. C., Nutman, A. P., Friend, C. R., Norman, M. D., Yaxley, G., 2009. Evidence for subduction at 3.8 Ga: geochemistry of arc-like metabasalts from the southern edge of the Isua Supracrustal Belt.*Chemical Geology*, *261*, 83–98.

Johnson, T.E., Brown, M., Kaus, B., VanTongeren, J.A., 2014. Delamination and recycling of Archean crust caused by gravitational instabilities. Nature Geoscience, 7, 47–52.

Johnson, T.E., Fischer, S., White, R.W., 2013. Field and petrographic evidence for partial melting of TTG gneiss within the central region of the mainland Lewisian complex, NW Scotland. Journal of the Geological Society, London, 170, 319–326.

Johnson, T.E., Fischer, S., White, R.W., Brown, M., Rollinson, H.R., 2012. Archean intracrustal differentiation from partial melting of metagabbro – field and geochemical evidence from the central region of the Lewisian complex, NW Scotland. Journal of Petrology, 53, 2115–2138.

Johnson, T.E., White, R.W., 2011. Phase equilibrium constraints on conditions of granulite-facies metamorphism at Scourie, NW Scotland. Journal of the Geological Society, London, 168, 147–158.

Kerrich, R., Polat, A., Wyman, D., Hollings, P., 1999. Trace element systematics of Mg-, to Fe-tholeiitic basalt suites of the Superior Province: implications for Archean mantle reservoirs and greenstone belt genesis. Lithos, 46, 163-187.

Kinny, P.D., Friend, C.R.L., 1997. U–Pb isotopic evidence for the accretion of different crustal blocks to form the Lewisian complex of northwest Scotland. Contributions to Mineralogy and Petrology, 129, 326–340.

Kinny, P.D., Friend, C.R.L., Love, G.J., 2005. Proposal for a terrane-based nomenclature for the Lewisian Gneiss Complex of NW Scotland. Journal of the Geological Society, London, 162. 175–186.

Kisters, A. F., & Anhaeusser, C. R., 1995. Emplacement features of Archean TTG plutons along the southern margin of the Barberton greenstone belt, South Africa. Precambrian Research, 75, 1–15.

Kisters, A.F.M., Stevens, G., Dziggel, A., Armstrong, R.A., 2003. Extensional detachment faulting and core-complex formation in the southern Barberton granite–greenstone terrain, South Africa: Evidence for a 3.2 Ga orogenic collapse: Precambrian Research, 127, 355–378.

Kisters, A.F.M., Belcher, R.W., Poujol, M., Dziggel, A., 2010. Continental growth and convergence-related arc plutonism in the MesoArchean: Evidence from the Barberton granitoid–greenstone terrain, South Africa: Precambrian Research, 178, 15–26.

Kuno, H., 1968. Differentiation of basalt magma. In: Hess, H.H., Poldervaart, A. (eds), Basalts: The Poldervaart treatise on rocks of basaltic composition, Vol. 2. Interscience, New York, pp. 623–688.

Le Maitre, R.W., Streckeisen, A., Zanettin, B., Le Bas, M.J., et al., 2002. Igneous Rocks: A Classification and Glossary of Terms, Recommendations of the International Union of Geological Sciences. Cambridge University Press, Cambridge, UK.

Li, C., Arndt, N.T., Tang, Q., Ripley, E.M., 2015. Trace element indiscrimination diagrams. Lithos, 232, 76–83.

Lin, S., Beakhouse, G.P., 2013. Synchronous vertical and horizontal tectonism at late stages of Archean cratonization and genesis of Hemlo gold deposit, Superior craton, Ontario, Canada. Geology, 41, 359–362.

Liou, J.G., Tsujimori, T., Yang, J., Zhang, R.Y., Ernst, W.G., 2014. Recycling of crustal materials through study of ultrahigh-pressure minerals in collisional orogens, ophiolites, and mantle xenoliths: A review. Journal of Asian Earth Sciences, 96, 386–420.

Love, G., Kinny, P., Friend, C., 2004. Timing of magmatism and metamorphism in the Gruinard Bay area of the Lewisian Gneiss Complex: comparisons with the Assynt Terrane and implications for terrane accretion. Contributions to Mineralogy and Petrology, 146, 620–636.

MacDonald, J.M., Wheeler, J., Harley, S.L., Mariani, E., Goodenough, K.M., Crowley, Q., Tatham, D., 2013. Lattice distortion in a zircon population and its effects on trace element mobility and U–Th–Pb isotope systematics: examples from the Lewisian

Gneiss Complex, northwest Scotland. Contributions to Mineralogy and Petrology, 166, 21–41.

Marshak, S., 1999. Deformation style way back when: thoughts on the contrasts between Archean/Paleoproterozoic and contemporary orogens. Journal of Structural Geology, 21, 1175–1182.

Martin, H., Moyen, J.-F, Guitreau, M., Blichert-Toft, J., Le Pennec, J.-L., 2014. Why Archean TTG cannot be generated by MORB melting in subduction zones. Lithos, 198–199, 1–13.

Mason, A. J., 2015. The Palaeoproterozoic anatomy of the Lewisian Complex, NW Scotland: evidence for two 'Laxfordian' tectonothermal cycles. Journal of the Geological Society, xx, xxx–xxx.

McDonough, W.F., Sun, S.-s., 1995. The composition of the Earth. Chemical Geology, 120, 223–253.

McGregor, A.M., 1951. Some milestones in the Precambrian of Southern Rhodesia. Geological Society of South Africa Transactions and Proceedings, 54, 27–71.

Moorbath, S., Welke, H., Gale, N., 1969. The significance of lead isotope studies in ancient, high-grade metamorphic basement complexes, as exemplified by the Lewisian rocks of Northwest Scotland. Earth and Planetary Science Letters, 6, 245–256.

Moyen, J.-F., 2011. The composite Archean grey gneisses: Petrological significance, and evidence for a non-unique tectonic setting for Archean crustal growth. Lithos, 123, 21–36.

Moyen, J.-F., Martin, H., 2012. Forty years of TTG research. Lithos, 148, 312-336.

Myers, J. S., Watkins, K. P., 1985. Origin of granite–greenstone patterns, Yilgarn Block, Western Australia. Geology, 13, 778–780.

Nutman, A.P., Bennett, V.C., Friend, C.R.L., Hidaka, H., Yi, K., Lee, S.R., Kamiichi, T.,

2013. The Itsaq gneiss complex of Greenland: episodic 3900 to 3660 Ma juvenile crust formation and recycling in the 3660 to 3600 Ma Isukasian orogeny. American Journal of Science, 313, 877–911.

Nutman, A.P., Bennett, V.C., Friend, C.R.L., 2015. The emergence of the Eoarchaean proto-arc: evolution of a c. 3700 Ma convergent plate boundary at Isua, southern West Greenland. Geological Society Special Publication, 389, 113–133.

O'Hara, M.J., 1961. Zoned Ultrabasic and Basic Gneiss Masses in the Early Lewisian Metamorphic Complex at Scourie, Sutherland. Journal of Petrology, 2, 248–276.

O'Hara, M.J., 1965. Origin of ultrabasic and basic masses in the Lewisian. Geological Magazine, 102, 296–314.

O'Hara, M.J., 1966. Correspondence. Origin of ultrabasic and basic masses in the Lewisian. Geological Magazine, 103, 284.

O'Hara, M.J., Yarwood, G., 1978. High pressure–temperature point on an Archean geotherm, implied magma genesis by crustal anatexis, and consequences for garnet-pyroxene thermometry and barometry. Philosophical Transactions of the Royal Society of London. Series A, Mathematical and Physical Sciences, 288, 441–456.

O'Nions, R. K., Hamilton, P. J., & Hooker, P. J., 1983. A Nd isotope investigation of sediments related to crustal development in the British Isles. Earth and Planetary Science Letters, 63, 229–240.

Ordóñez-Calderón, J.C., Polat, A., Fryer, B.J., Gagnon, J.E., 2011. Field and geochemical characteristics of Mesoarchean to Neoarchean volcanic rocks in the Storø greenstone belt, SW Greenland: Evidence for accretion of intra-oceanic volcanic arcs. Precambrian Research, 184, 24-42.

Qian, Q., Hermann, J., 2013. Partial melting of lower crust at 10–15 kbar: constraints on adakite and TTG formation. Contributions to Mineralogy and Petrology, 165, 1195–

1224.

Park, R.G., 2005. The Lewisian terrane model: a review. Scottish Journal of Geology, 41, 105–118.

Park, R.G., 1970. Observations on Lewisian Chronology. Scottish Journal of Geology, 6, 379–399.

Park, R.G., Tarney, J., 1987. The Lewisian complex: a typical Precambrian high-grade terrain? In: Park, R. G., Tarney, J. (eds) Evolution of the Lewisian and Comparable Precambrian High Grade Terrains. Geological Society, London, Special Publications, 27, 13–25.

Park, R.G., Tarney, J., Connelly, J. N., 2001. The Loch Maree Group: Palaeoproterozoic subduction-accretion complex in the Lewisian of NW Scotland. Precambrian Research, 105, 205–226.

Parmenter, A.C., Lin, S.F., Corkery, M.T., 2006. Structural evolution of the Cross Lake greenstone belt in the northwestern Superior Province, Manitoba: implications for relationship between vertical and horizontal tectonism. Canadian Journal of Earth Sciences, 43, 767–787.

Peach, B. N., Horne, J., Gunn, W., Clough, C. T., Hinxman, L. W., Teall, J. J. H., 1907. The Geological Structure of the North West Highlands of Scotland, Memoirs of the Geological Survey of Great Britain.

Pearce, J.A., 2008. Geochemical fingerprinting of oceanic basalts with applications to ophiolite classification and the search for Archean oceanic crust. Lithos, 100, 14–48.

Pearce, J.A., 2014a. Geochemical Fingerprinting of the Earth's Oldest Rocks. Geology, 42, 175–176.

Pearce, J.A., 2014b. Immobile element fingerprinting of ophiolites. Elements, 10, 101–108.

Pearce, J.A., Cann, J.R., 1973. Tectonic setting of basic volcanic rocks determined using trace element analyses. Earth and Planetary Science Letters, 19, 290–300.

Pearce, J.A., Peate, D.W., 1995. Tectonic implications of the composition of volcanic arc magmas. Annual Review of Earth and Planetary Sciences, 23, 251–285.

Polat, A., 2009. The geochemistry of Neoarchean (ca. 2700 Ma) tholeiitic basalts, transitional to alkaline basalts, and gabbros, Wawa Subprovince, Canada: Implications for petrogenetic and geodynamic processes. Precambrian Research, 168, 83-105.

Polat, A., Wang, L., Appel, P. W., 2015. A review of structural patterns and melting processes in the Archean craton of West Greenland: Evidence for crustal growth at convergent plate margins as opposed to non-uniformitarian models. Tectonophysics, xx, xxx–xxx.

Pride, C., Muecke, G.K., 1982. Geochemistry and origin of granitic rocks, Scourian Complex, NW Scotland. Contributions to Mineralogy and Petrology, 80. 379–385.

Pride, C., Muecke, G.K., 1980. Rare earth element geochemistry of the Scourian complex N.W. Scotland – Evidence for the granite-granulite link. Contributions to Mineralogy and Petrology, 73, 403–412.

Ramsay, J.G., 1989. Emplacement kinematics of a granite diapir: the Chindamora batholith, Zimbabwe. Journal of Structural Geology, 11, 191–209.

Rapp, R. P., Shimizu, N., & Norman, M. D., 2003. Growth of early continental crust by partial melting of eclogite. Nature, 425, 605–609.

Robin, C.M.I., Bailey, R.C., 2009. Simultaneous generation of Archean crust and subcratonic roots by vertical tectonics. Geology, 37, 523–526.

Rollinson, H.R., 1996. Tonalite-trondhjemite-granodiorite magmatism and the genesis of Lewisian crust during the Archean. In: Brewer, T.S. (ed). Precambrian Crustal Evolution in the North Atlantic Region. Geological Society, London, Special Publications, 112, 25–42.

Rollinson, H., 2012. Geochemical constraints on the composition of Archean lower continental crust: Partial melting in the Lewisian granulites. Earth and Planetary Science Letters, 351–352, 1–12.

Rollinson, H.R., Fowler, M.B., 1987. The magmatic evolution of the Scourian complex at Gruinard Bay. In: Park, R. G. and Tarney, J. (eds) Evolution of the Lewisian and Comparable Precambrian High Grade Terrains. Geological Society, London, Special Publications, 27, 57–71.

Rollinson, H.R., Gravestock, P., 2012. The trace element geochemistry of clinopyroxenes from pyroxenites in the Lewisian of NW Scotland: insights into light rare earth element mobility during granulite facies metamorphism. Contributions to Mineralogy and Petrology, 163, 319–335.

Rollinson, H.R., Tarney, J., 2005. Adakites – the key to understanding LILE depletion in granulites. Lithos, 79, 61–81.

Rollinson, H.R., Windley, B.F., 1980. An Archean granulite-grade tonalite–trondhjemite–granite suite from Scourie, NW Scotland: Geochemistry and origin. Contributions to Mineralogy and Petrology, 72, 265–281.

Sandiford, M., Kranendonk, M.V., Bodorkos, S., 2004. Conductive incubation and the origin of Granite-Greenstone dome-and-keel structure: the eastern Pilbara Craton. Tectonics, 23, TC1009, doi:10.1029/2002TC001452.

Sajeev, K., Windley, B.F., Hegner, E., Komiya, T., 2013. High-temperature, high-pressure granulites (retrogressed eclogites) in the central region of the Lewisian, NW Scotland: Crustal-scale subduction in the NeoArchean. Gondwana Research, 23, 526–538.

Sheraton, J.W., Tarney, J., Wheatley, T.J., Wright, A.E., 1973. The Structural History of the Assynt district. In: Park, R.G and Tarney, J. (eds) The Early Precambrian of Scotland and Related Rocks of Greenland. University of Keele, pp. 31–43.

Sills, J.D., 1983. Mineralogical changes occurring during the retrogression of Archean gneisses from the Lewisian complex of NW Scotland. Lithos, 16, 113–124.

Sills, J.D., Rollinson, H.R., 1987. Metamorphic evolution of the mainland Lewisian complex. In: Park, R. G. and Tarney, J. (eds) Evolution of the Lewisian and Comparable Precambrian High Grade Terrains. Geological Society, London, Special Publications, 27, 81–92.

Sills, J.D., Savage, D., Watson, J.V., Windley, B.F., 1982. Layered ultramafic-gabbro bodies in the Lewisian of northwest Scotland: geochemistry and petrogenesis, Earth and Planetary Science Letters, 58, 345–360.

Snow, C., 2006. A reevaluation of tectonic discrimination diagrams and a new probabilistic approach using large geochemical databases: moving beyond binary and ternary plots. Journal of Geophysical Research, 111, http://dx.doi.org/10.1029/2005JB003799 (B06206).

Sizova, E., Gerya, T., Stüwe, K., Brown, M., 2015. Generation of felsic crust in the Archean: a geodynamic modeling perspective. Precambrian Research, revised awaiting acceptance.

Sun, S.s., McDonough, W.F., 1989. Chemical and isotopic systematics of oceanic basalts: implications for mantle composition and processes. In: Saunders, A.D., Norry, M.J. (eds) Magmatism in the Ocean Basins. Geological Society, London, Special Publications, 42, 313–345.

Sutton, J., Watson, J., 1951. The pre-Torridonian metamorphic history of the Loch Torridon and Scourie areas in the North-West Highlands, and its bearing on the chronological classification of the Lewisian. Quarterly Journal of the Geological Society, 106, 241–307.

Tatsumi, Y. (2005). The subduction factory: how it operates in the evolving Earth. *GSA* *today*, *15*, 4.

Thebaud, N., Rey, P.F., 2013. Archean gravity-driven tectonics on hot and flooded continents: Controls on long-lived mineralised hydrothermal systems away from continental margins. Precambrian Research, 229, 93–104.

Van Kranendonk, M.J., Collins, W.J., Hickman, A., Pawley, M.J., 2004. Critical tests of vertical vs. horizontal tectonic models for the Archean East Pilbara Granite-Greenstone Terrane, Pilbara Craton, Western Australia. Precambrian Research, 131, 173–211.

Van Kranendonk, M.J., Kröner, A., Hoffman, E.J., Nagel, T., Anhaeusser, C.R., 2014. Just another drip: re-analysis of a proposed Mesoarchean suture from the Barberton Mountain Land, South Africa. Precambrian Research, 254, 19–35.

Walter, M.J., 1998. Melting of Garnet Peridotite and the Origin of Komatiite and Depleted Lithosphere. Journal of Petrology, 39, 29–60.

Weaver, B.L., Tarney, J., 1980. Rare earth geochemistry of Lewisian granulite-facies gneisses, northwest Scotland: Implications for the petrogenesis of the Archean lower continental crust. Earth and Planetary Science Letters, 51, 279–296.

Wellman, P., 2000. Upper crust of the Pilbara Craton, Australia; 3D geometry of a granite/greenstone terrain. Precambrian Research, 104, 175–186.

Wheeler, J., 2007. A major high strain zone in the Lewisian Complex in the Loch Torridon area, NW Scotland: insights into deep crustal deformation. In: Ries, A.C., Butler, R.W.H., Graham, R.H. (eds) Deformation of the Continental Crust: The Legacy of Mike Coward. Geological Society, London, Special Publications, 272, 27–45.

Wheeler, J., Park, R.G., Rollinson, H.R., Beach, A., 2010. The Lewisian Complex: insights into deep crustal evolution. In: Law, R., Butler, R.W.H., Holdsworth, R.E., Krabbendam, M., Strachan, R. (eds) Continental Tectonics and Mountain Building: The Legacy of Peach and Horne. Geological Society, London, Special Publications, 335, 51–79.

Whitehouse, M.J., 1989. Sm–Nd evidence for diachronous crustal accretion in the Lewisian complex of northwest Scotland. Tectonophysics, 161, 245–256.

Whitehouse, M.J., Claesson, S., Sunde, T., Vestin, J., 1997. Ion microprobe U-Pb zircon geochronology and correlation of Archean gneisses from the Lewisian Complex of Gruinard Bay, northwestern Scotland. Geochimica et Cosmochimica Acta, 61, 4429–4438.

Whitehouse, M.J., Fowler, M.B., Friend, C.R.L., 1996. Conflicting mineral and whole-rock isochron ages from the Late-Archean Lewisian complex of northwestern Scotland: Implications for geochronology in polymetamorphic high-grade terrains. Geochimica et Cosmochimica Acta, 60, 3085–3102.

Whitehouse, M.J., Kemp, A.I.S., 2010. On the difficulty of assigning crustal residence, magmatic protolith and metamorphic ages to Lewisian granulites: constraints from combined in situ U-Pb and Lu-Hf isotopes. In: Law, R., Butler, R.W.H., Holdsworth, R.E., Krabbendam, M., Strachan, R. (eds) Continental Tectonics and Mountain Building: The Legacy of Peach and Horne. Geological Society, London, Special Publications, 335, 81–101.

Windley, B. F., Bridgwater, D., 1971. The evolution of Archean low- and high-grade terrains. Geological Society of Australia, Special Publication, 3, 33–46.

Windley, B. F., Smith, J.V., 1971. Archean high-grade complexes and modern continental margins. Nature, 260, 671–675.

Zhang, C., Holtz, F., Koepke, J., Wolff, P.E., Ma, C., Bédard, J.H., 2013. Constraints from experimental melting of amphibolite on the depth of formation of garnet-rich restites, and implications for models of Early Archean crustal growth. Precambrian Research, 231, 206–217.

Zhu, Z.K., O'Nions, R.K., Belshaw, N.S., Gibb, A.J., 1997. Lewisian crustal history from in situ SIMS mineral chronometry and related metamorphic textures. Chemical Geology, 136, 205–218.

Zirkler, A., Johnson, T.E., White, R.W., Zack, T., 2012. Polymetamorphism in the mainland Lewisian complex, NW Scotland – phase equilibria and geochronological constraints from the Cnoc an t'Sidhean suite. Journal of Metamorphic Geology, 30, 865.

**Figure captions**

**Fig. 1.** A simplified geological map of the mainland Lewisian Complex of northwest Scotland. The complex is traditionally subdivided into a granulite facies central region bounded by the mainly amphibolite facies northern and southern regions. The more recent terrane-based nomenclature is also shown (the Gruinard and Assynt terranes in the center, with the Rhiconich terrane to the north and the Gairloch, Ialltaig and Rona terranes to the south; Kinny et al., 2005). The position of key localities discussed in the text is indicated.

**Fig. 2.** (a) Geological map, reproduced with permission of the BGS (Innovation agreement IPR/156–04CL), showing the distribution of the main rocks types in the northwestern part of the central region (Assynt block), across the Laxford Shear Zone (LSZ) and into the southwesternmost part of the northern region (Rhiconich block). The map is based on recent BGS mapping with the location of additional ultramafic–mafic bodies from fig. 1 of Davies (1976) superimposed (dashed boundaries). The boundaries of the LSZ (approximate positions shown by the two thick dotted grey lines) trend WNW–ESE and pass through the middle of Loch Laxford in the north and 2–3 km northeast of Scourie in the south, where the strain gradient declines and the strain becomes localized in discrete shear zones. The precise junction between the central and northern regions is unclear. West and south of the Laxford granites, a prominent belt of large layered ultramafic–mafic bodies is spatially associated with brown gneisses that occur in synformal cores. By contrast, many of the more isolated layered bodies, for instance around Scourie, have no clear association with brown gneiss. The schematic cross-section (b), redrafted from Davies (1976), was drawn along the line A–B indicated on the map.

**Fig. 3.** Timeline based on data cited in the main text summarising the age constraints on Archean to Paleoproterozoic ‘events’ within the central region of the mainland Lewisian Complex.

**Fig. 4.** (a) Generalized stratigraphy of the layered ultramafic–mafic bodies and associated supracrustal rocks; (b) Field photographs of typical occurrences of the various units shown in (a); (c) Chondrite-normalised REE patterns of the various units shown in (a) and (b). In (c), the grey background field for the brown gneisses shows the range of compositions of petrographically similar garnet–biotite gneisses from the Storø greenstone belt, SW Greenland (Ordóñez-Calderón et al., 2011). The grey background field for the ultramafic rocks shows the range of REE compositions for ~200 komatiites from greenstone belts in the Superior Province taken from the GEOROC database (http://georoc.mpch-mainz.gwdg.de/).

**Fig. 5.** Variation diagrams showing major oxide compositions of the main lithologies plotted against MgO (as wt%). The compositions of Archean non-arc basalts, Archean basalts from the Superior and North Atlantic cratons (SNAC basalts), N-MORB and fertile mantle composition KR–4003 are shown for reference, along with the average composition of olivine (ol) and clinopyroxene (cu) from a metamorphosed ultramafic rock and of clinopyroxene (cm) from a metabasic rock – see main text for further details.

**Fig. 6.** (a) AFM diagram showing the boundaries between the tholeiitic and calc-alkaline fields proposed by Kuno (1968) and Irvine and Baragar (1971). The ultramafic and metabasic rocks define a low-alkali trend with strong enrichment in Fe that is characteristic of tholeiitic magmas. (b) TAS diagram showing the compositions of the metabasic rocks and brown gneisses.

**Fig. 7.** Representative trace element compositions of the main lithologies normalised to primitive mantle values of McDonough & Sun (1995). The grey areas show the fields for particular reference compositions described in the text.

**Fig. 8.** Change in the major (Si to K as oxides) and trace element composition of the average metabasic rock relative to the average SNAC basalt. Many of these features (e.g. a depletion in K, Na and most trace elements) are consistent with partial melting and melt loss. Others (e.g. the pronounced depletion in Ti, Nb and Ta) probably reflect source characteristics (e.g. Rollinson, 2012).

**Fig. 9.** Trace element discrimination diagrams: (a) Nb/Y vs Ti/Y; (b) Nb/Yb vs Th/Yb; (c) Nb/Yb vs $TiO_2$/Yb.

Highlights

- The Lewisian Complex contains large layered ultramafic–mafic bodies and structurally overlying garnet-biotite gneiss whose origin is unclear
- The rocks have ‘arc-like’ geochemical signatures that may not be unique to a subduction environment
- The ultramafic–mafic rocks and brown gneisses may represent the remnants of intracratonic greenstone belts that sank into the deep crust due to their density contrast with the underlying partially molten low viscosity TTG orthogneisses

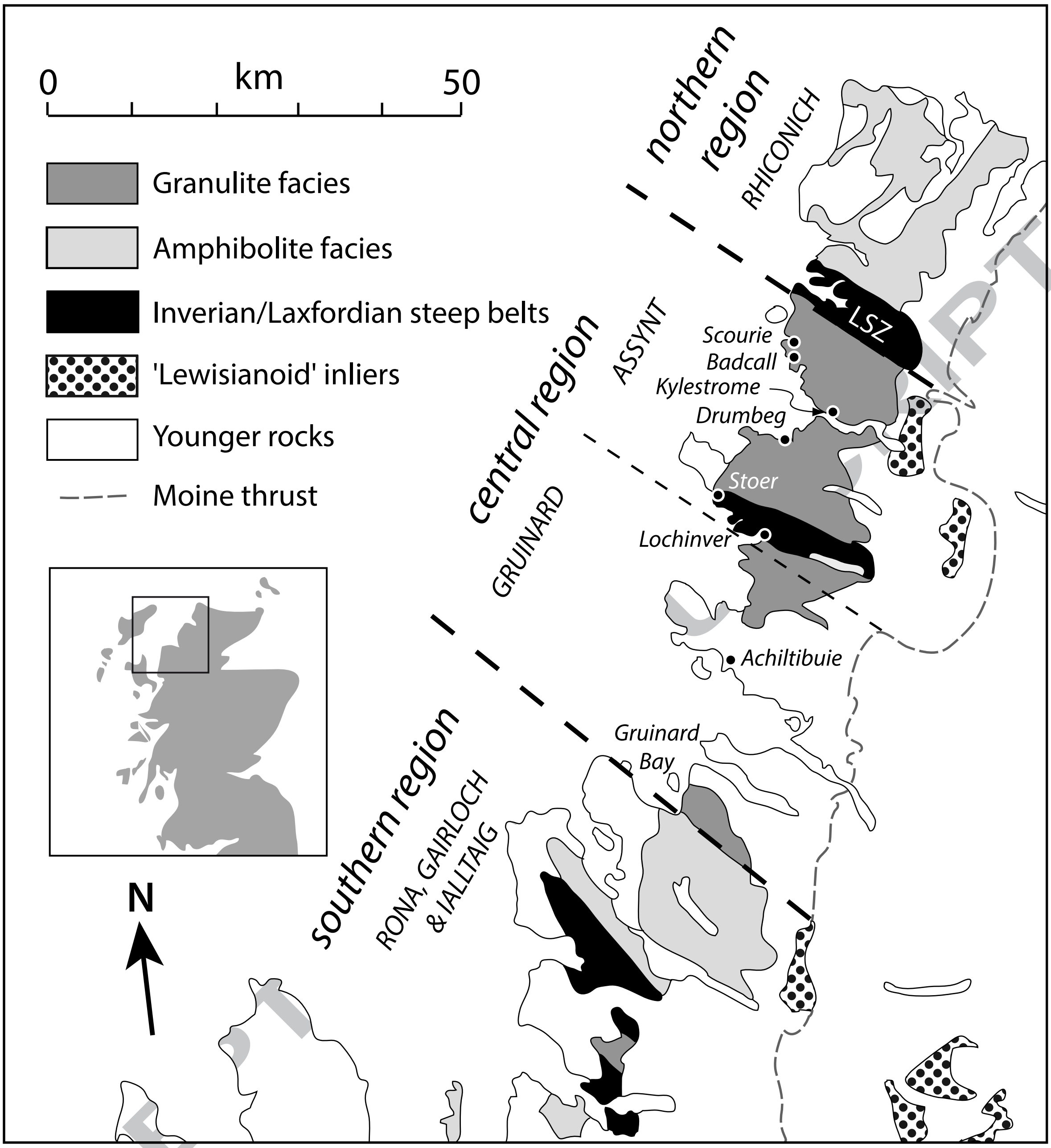
0
km
50
Granulite facies
Amphibolite facies
Inverian/Laxfordian steep belts
'Lewisianoid' inliers
Younger rocks
Moine thrust
N
northern region
RHICONICH
central region
ASSYNT
GRUINARD
southern region
RONA, GAIRLOCH & IALLTAIG
LSZ
Scourie
Badcall
Kylestrome
Drumbeg
Stoer
Lochinver
Achiltibuie
Gruinard Bay

Figure 1

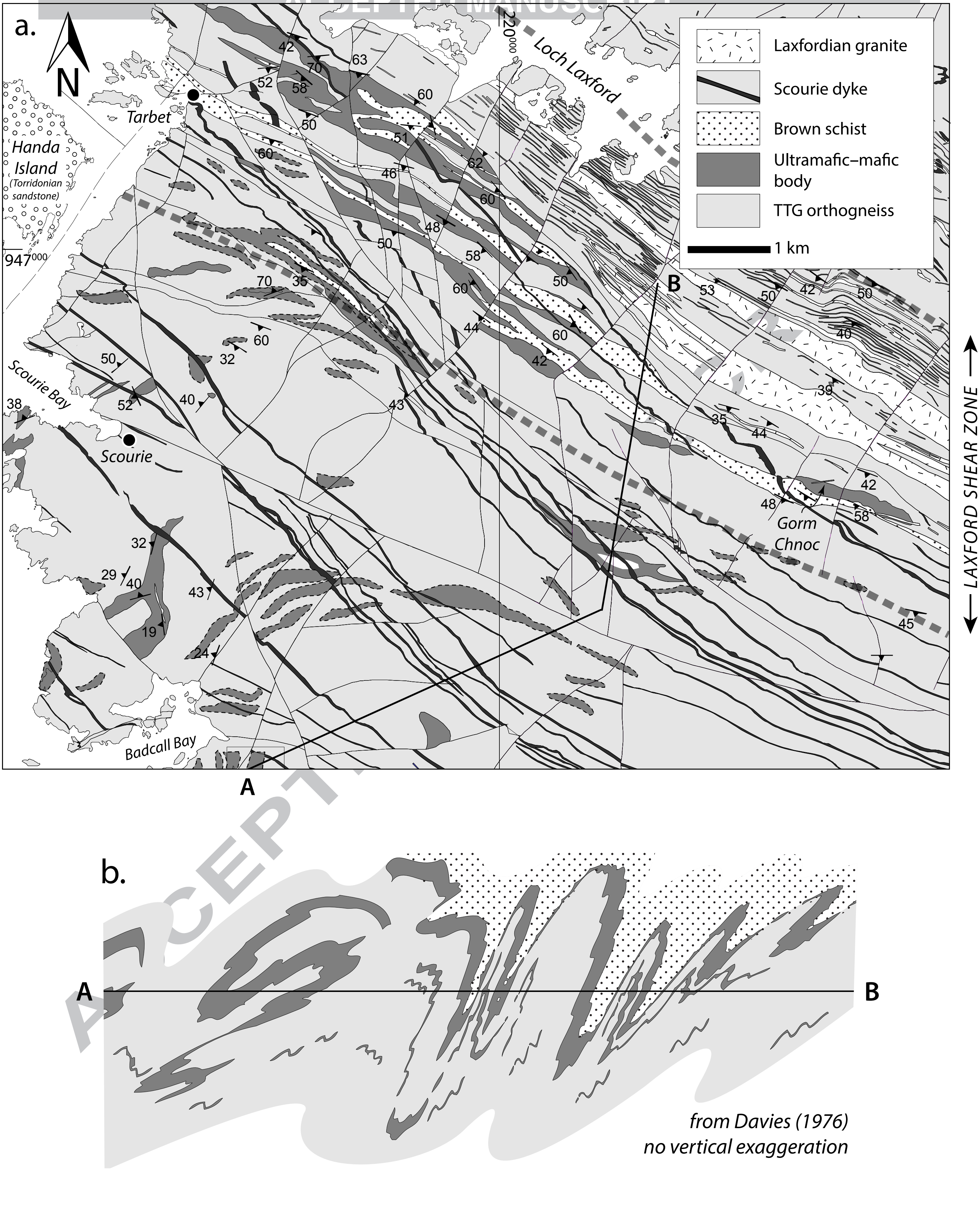
a.
N
Laxfordian granite
Scourie dyke
Brown schist
Ultramafic–mafic body
TTG orthogneiss
1 km
Loch Laxford
Tarbet
Handa Island
(Torridonian sandstone)
Scourie Bay
Scourie
Badcall Bay
Gorm Chnoc
LAXFORD SHEAR ZONE
A
B
b.
from Davies (1976)
no vertical exaggeration

Figure 2

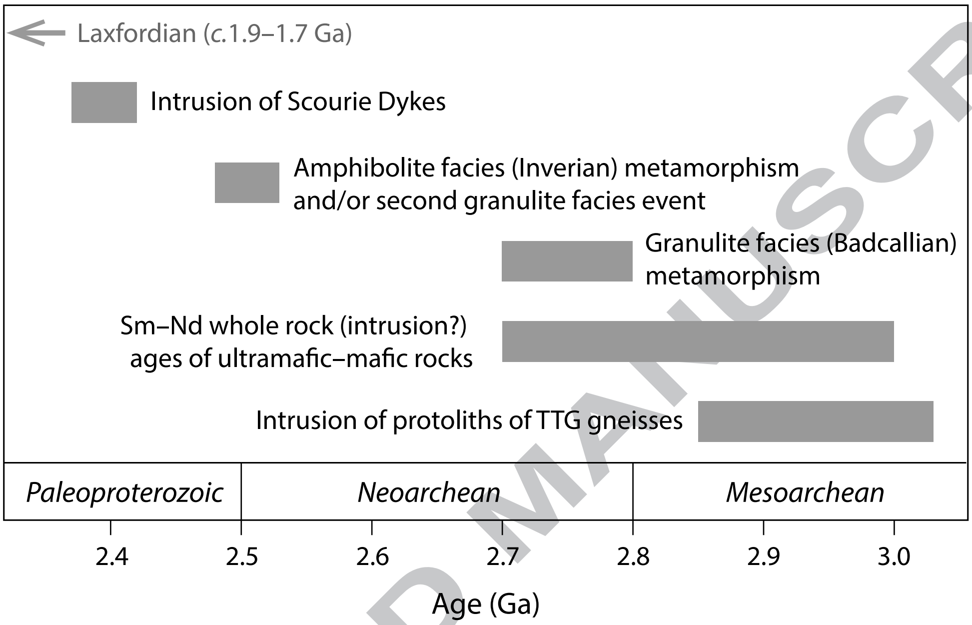
Laxfordian (c.1.9–1.7 Ga)
Intrusion of Scourie Dykes
Amphibolite facies (Inverian) metamorphism and/or second granulite facies event
Granulite facies (Badcallian) metamorphism
Sm–Nd whole rock (intrusion?) ages of ultramafic–mafic rocks
Intrusion of protoliths of TTG gneisses
Paleoproterozoic
Neoarchean
Mesoarchean
2.4
2.5
2.6
2.7
2.8
2.9
3.0
Age (Ga)

Figure 3

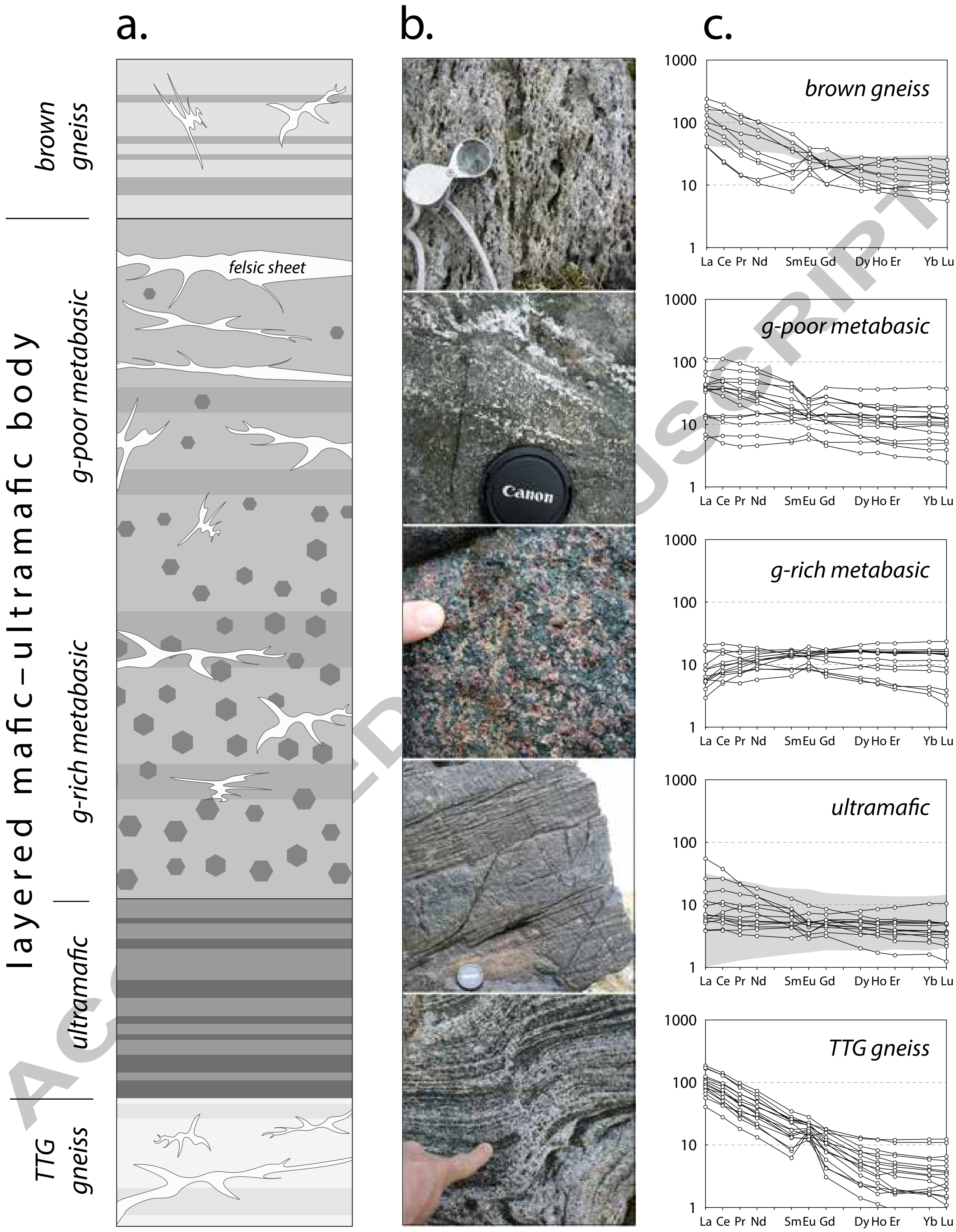
a.
b.
c.
brown gneiss
layered mafic–ultramafic body
g-poor metabasic
g-rich metabasic
ultramafic
TTG gneiss
felsic sheet
Canon
1000
100
10
1
La Ce Pr Nd Sm Eu Gd Dy Ho Er Yb Lu
brown gneiss
g-poor metabasic
g-rich metabasic
ultramafic
TTG gneiss

Figure 4

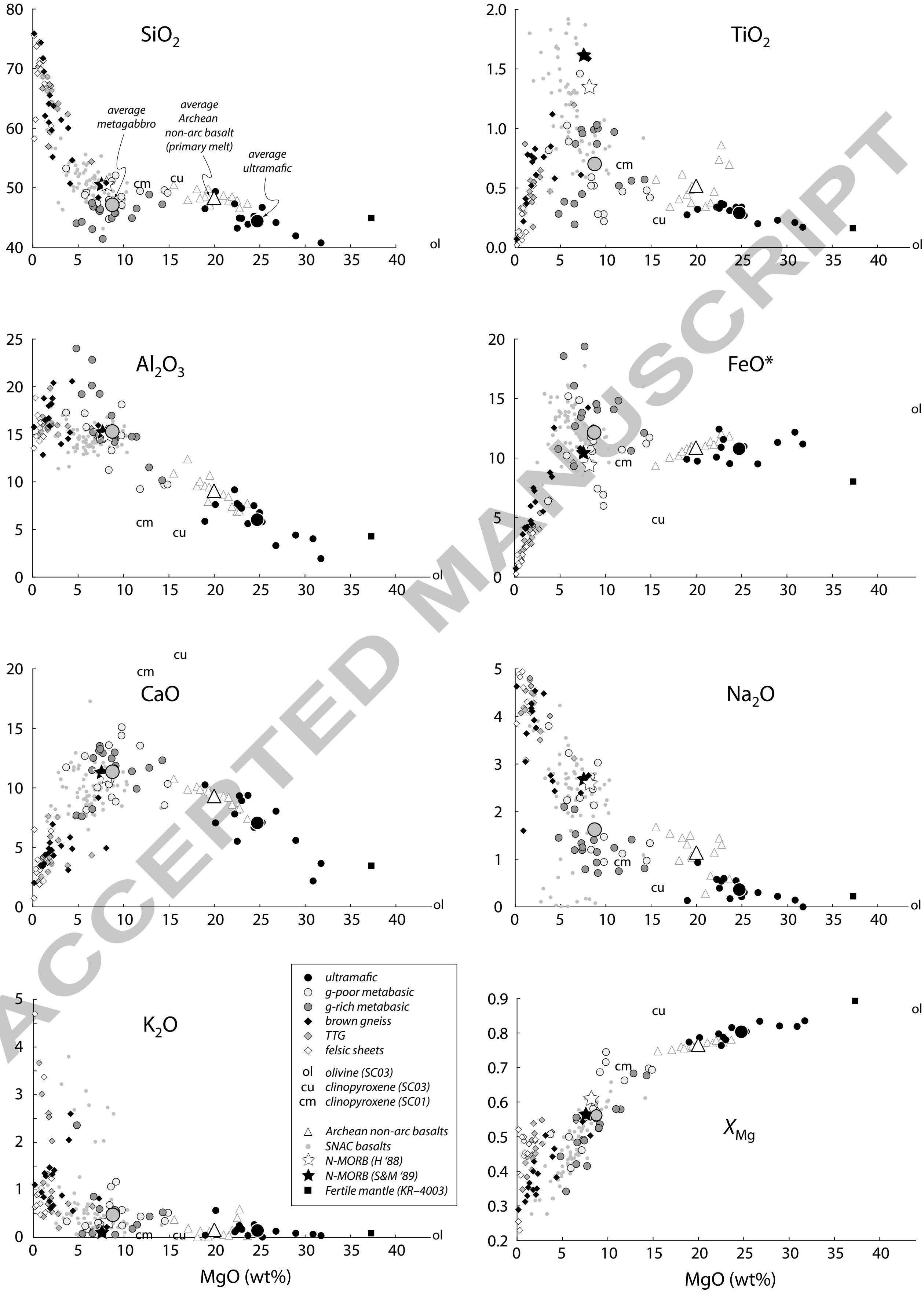
SiO$_2$
average metagabbro
average Archean non-arc basalt (primary melt)
average ultramafic
TiO$_2$
Al$_2$O$_3$
FeO*
CaO
Na$_2$O
K$_2$O
$X_{Mg}$
cm
cu
ol
MgO (wt%)
ultramafic
g-poor metabasic
g-rich metabasic
brown gneiss
TTG
felsic sheets
ol olivine (SC03)
cu clinopyroxene (SC03)
cm clinopyroxene (SC01)
Archean non-arc basalts
SNAC basalts
N-MORB (H '88)
N-MORB (S&M '89)
Fertile mantle (KR–4003)

Figure 5

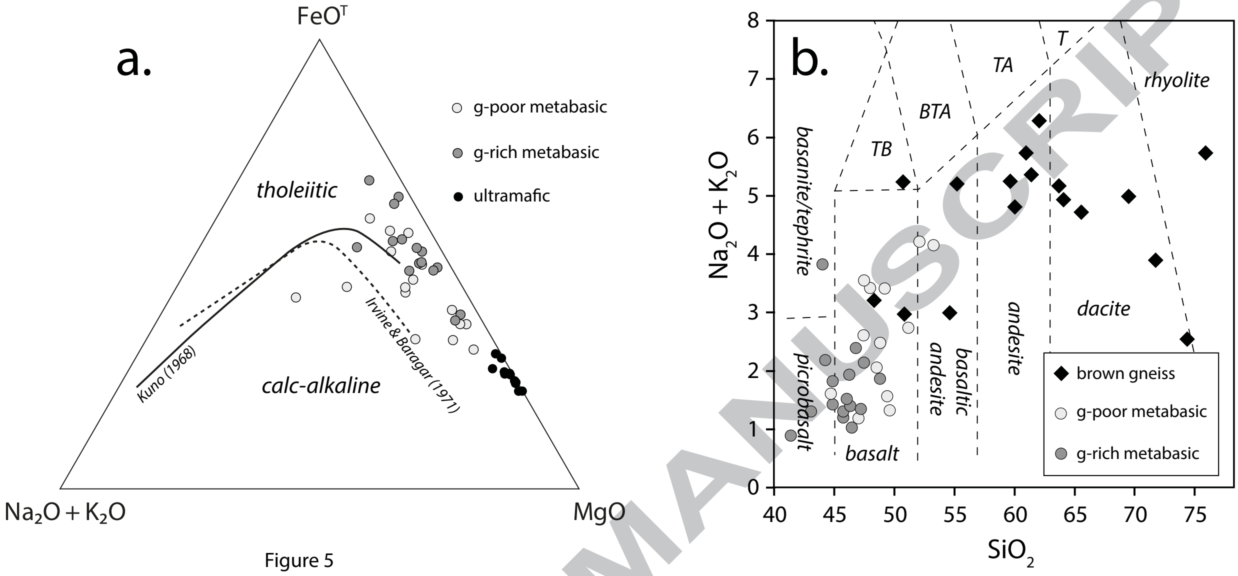
a.
FeO^T
g-poor metabasic
g-rich metabasic
ultramafic
tholeiitic
calc-alkaline
Kuno (1968)
Irvine & Baragar (1971)
Na2O + K2O
MgO
Figure 5
b.
8
7
6
5
4
3
2
1
0
Na2O + K2O
40
45
50
55
60
65
70
75
SiO2
TB
BTA
TA
T
rhyolite
basanite/tephrite
picrobasalt
basalt
basaltic andesite
andesite
dacite
brown gneiss
g-poor metabasic
g-rich metabasic

Figure 6

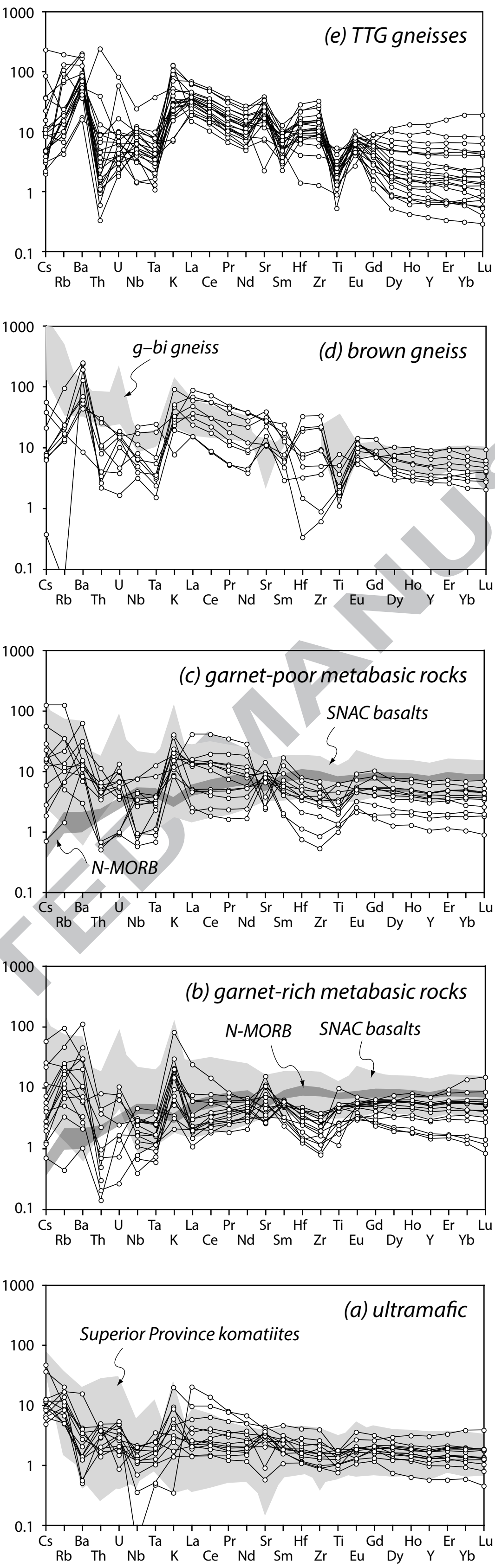

(e) TTG gneisses
(d) brown gneiss
g–bi gneiss
(c) garnet-poor metabasic rocks
SNAC basalts
N-MORB
(b) garnet-rich metabasic rocks
N-MORB
SNAC basalts
(a) ultramafic
Superior Province komatiites
1000
100
10
1
0.1
Cs Ba U Ta La Pr Sr Hf Ti Gd Ho Er Lu
Rb Th Nb K Ce Nd Sm Zr Eu Dy Y Yb


Figure 7

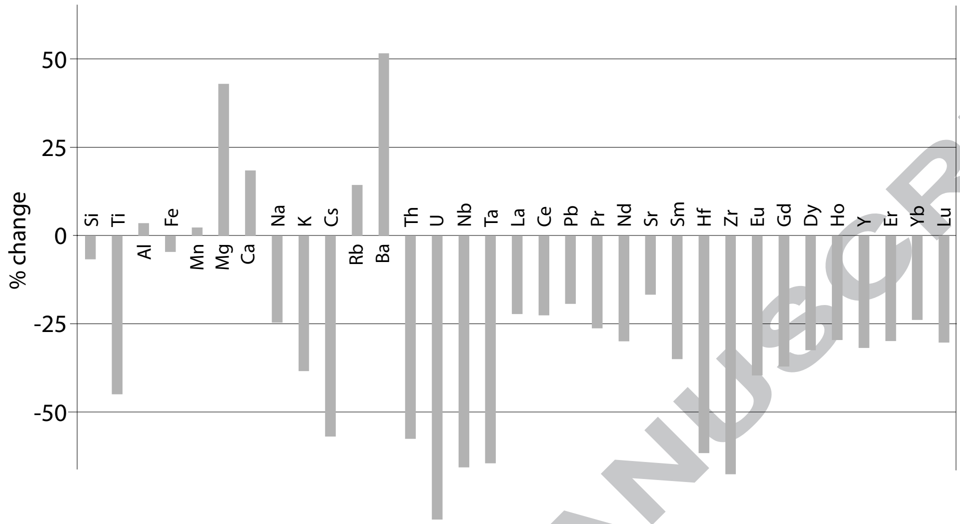
% change
50
25
0
-25
-50
Si
Ti
Al
Fe
Mn
Mg
Ca
Na
K
Cs
Rb
Ba
Th
U
Nb
Ta
La
Ce
Pb
Pr
Nd
Sr
Sm
Hf
Zr
Eu
Gd
Dy
Ho
Y
Er
Yb
Lu

Figure 8

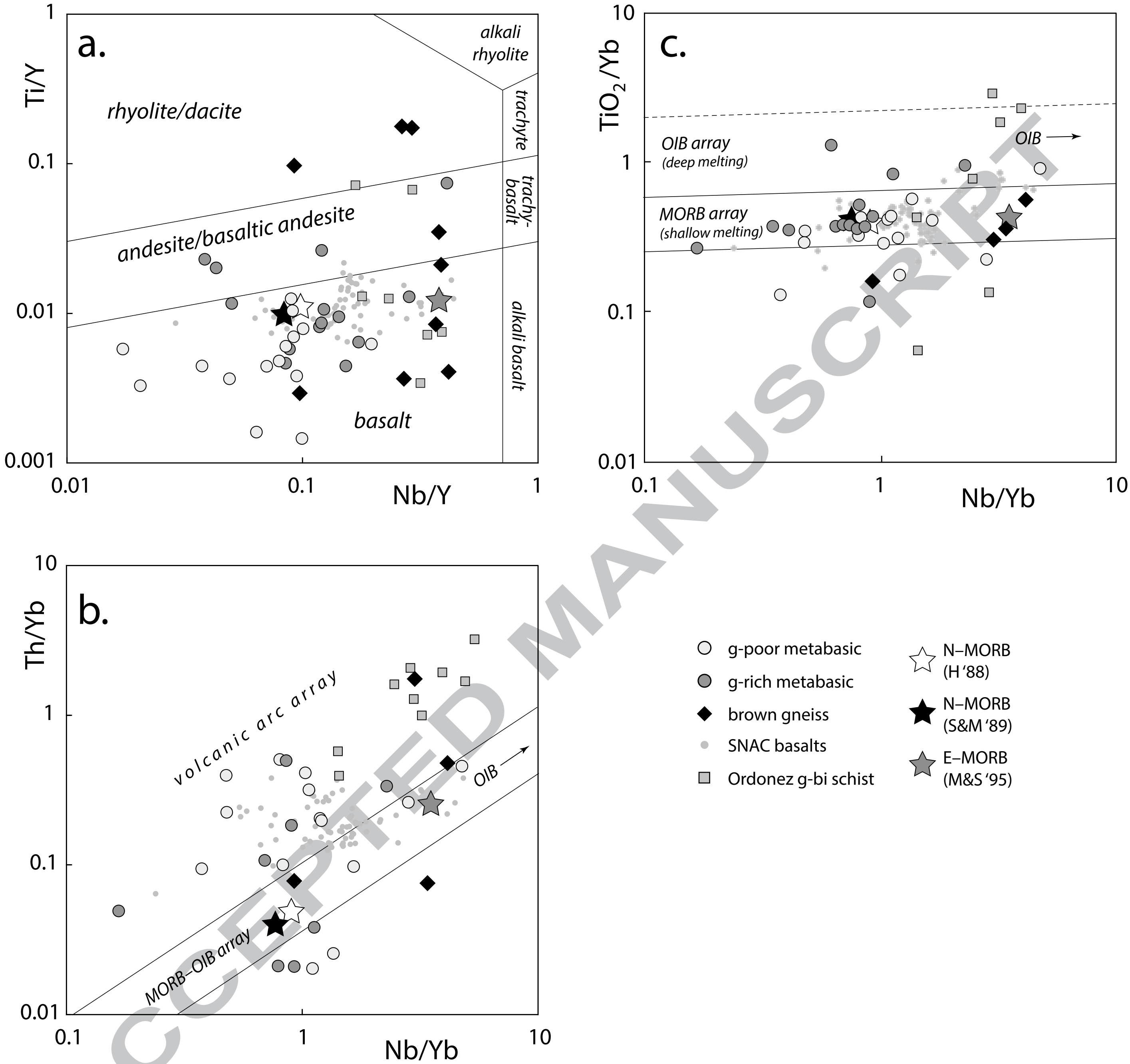
a.
Ti/Y
Nb/Y
1
0.1
0.01
0.001
0.01
0.1
1
alkali rhyolite
rhyolite/dacite
trachyte
trachy-basalt
andesite/basaltic andesite
alkali basalt
basalt
c.
$TiO_2$/Yb
Nb/Yb
10
1
0.1
0.01
0.1
1
10
OIB array
(deep melting)
MORB array
(shallow melting)
OIB
b.
Th/Yb
Nb/Yb
10
1
0.1
0.01
0.1
1
10
volcanic arc array
MORB–OIB array
OIB
g-poor metabasic
g-rich metabasic
brown gneiss
SNAC basalts
Ordonez g-bi schist
N–MORB (H '88)
N–MORB (S&M '89)
E–MORB (M&S '95)

Figure 9